Evaluating epidemiological scenarios of isolation and further releases considering protection actions to control transmission of CoViD-19 in São Paulo State, Brazil

Hyun Mo Yang[1]*, Luis Pedro Lombardi Junior[2],
Fabio Fernandes Morato Castro[3], Ariana Campos Yang[4]

[1,2]UNICAMP – IMECC – DMA; Praça Sérgio Buarque de Holanda, 651;
CEP: 13083-859, Campinas, SP, Brazil

[3,4]HC-FMUSP; Av. Dr. Eneas Carvalho de Aguiar, 255;
CEP: 05403-000, São Paulo, SP, Brazil

emails: [1]hyunyang@ime.unicamp.br, [2]luispedro_jr@hotmail.com,
[3]ffmcastro@gmail.com, [4]arianacy@gmail.com

Abstract

A mathematical model was formulated based on nonlinear ordinary differential equations considering young (below 60 years old) and elder (above 60 years) subpopulations, aiming to describe the introduction, dissemination and control of new coronavirus in São Paulo State, Brazil. In São Paulo State, the first case of CoViD-19 was confirmed on 26 February, the first death due to CoViD-19 was registered on 16 March, on 24 March the São Paulo State authorities implemented the isolation of persons in non-essential activities, which is programmed to end on June 1. The deterministic model used the data collected in São Paulo State to estimate the model parameters to describe the current epidemiological status in the State under isolation. We concluded that the proportion in isolation influenced the number of new cases in around 9 days ahead. We evaluate the suitability of lockdown in São Paulo State and concluded that this extreme measure should be efficient if lower transmission is occurring among isolated persons. Nevertheless, the isolated persons must be released one day. Based on this model, we studied the potential epidemiological scenarios of release by varying the release proportions of young and elder persons. We evaluated three releases divided in equal proportions elapsed 14

*Corresponding author: tel: + 55 19 3521-6031

days between releases, and three strategies: the first release occurring on June 1, 15 and 23. We concluded that these three strategies are equivalent (little difference) in reducing the number of hospitalization due to severe CoViD-19 and deaths, due to presenting the effective reproduction number near one. However, if protection actions as using face mask and hygiene (washing hands, for instance) could be massively disseminated in the population, we concluded there health care system may not collapse.

Keywords: mathematical model; new coronavirus; pulses of isolation/quarantine and release; face mask and hygiene; lockdown

1 Introduction

Coronavirus disease 2019 (CoViD-19), which is caused by severe acute respiratory syndrome coronavirus 2 (SARS-CoV-2), a strain of the RNA-based SARS-CoV-1,was declared pandemic by World Health Organization (WHO) on March 11, 2020. The rapid spreading of SARS-CoV-2 (new coronavirus) is due to the fact that this virus can be transmitted by droplets that escape the lungs through coughing or sneezing and infect humans (direct transmission), or they are deposited in surfaces and infect humans when in contact with this contaminated surface (indirect transmission). The virus enters into susceptible persons through the nose, mouth, or eyes, and infects cells in the respiratory tract, being capable to release millions of new viruses. Like all RNA-based viruses, the new coronavirus tends to mutate faster than DNA-viruses, but lower than influenza viruses.

Currently, there is not a vaccine, neither effective treatment. Hence, isolation is the main, if not unique, way of controlling the dissemination of this virus in a population aiming the change in the natural history of disease propagation (this change is commonly known as the flattening curve of epidemics). The reason is that in serious cases due to new coronavirus infection, immune cells overreact and attack the lung cell causing acute respiratory disease syndrome and possibly death. In general, the fatality rate in elder patients (60 years or more) is much higher than the average.

However, the isolation as control measure arises an important question: are there reliable strategies to release these isolated persons aiming to avoid the retaken of its original progression of infection?

Mathematical models allow us to understand the progression of viral infections if the natural history of the disease is well documented. Based on this knowledge being improved as epidemics evolves, in [30] considered continuous isolation and release rates to describe new coronavirus epidemics, which was improved by considering intermittent pulses in isolation and releases in [31]. Here, we improve previous model allowing the transmission by mild CoViD-19 persons. Taking into account pulses in isolation and releases, we describe the current epidemiological scenario in São Paulo State, Brazil, by estimating the model parameters. Based on this current scenario, we study potential epidemiological scenarios arising from releases.

The paper is structured as follows. In Section 2, we introduce a model, which is numerically studied in Section 3. Discussions are presented in Section 4, and conclusions in Section 5.

2 Material and methods

In a community where SARS-CoV-2 (new coronavirus) is circulating, the risk of infection is greater in elder than young persons, as well as elder persons are under increased probability of being symptomatic and higher CoViD-19 induced mortality. Hence, the community is divided into two groups, composed by young (under 60 years old, denoted by subscript y), and elder (above 60 years old, denoted by subscript o) persons. The vital dynamics of this community is described by per-capita rates of birth (ϕ) and mortality (μ).

For each sub-population j ($j = y, o$), all persons are divided into nine classes: susceptible S_j, susceptible persons who are isolated Q_j, exposed and incubating E_j, asymptomatic A_j, asymptomatic persons who are caught by test and then isolated Q_{1j}, symptomatic persons at initial phase of CoViD-19 (or pre-diseased) D_{1j}, pre-diseased persons caught by test and then isolated, plus mild CoViD-19 (or non-hospitalized) Q_{2j}, symptomatic persons with severe CoViD-19 (hospitalized) D_{2j}, and non-hospitalized persons convinced to be isolated by educational campaign Q_{3j}. However, all young and elder persons in classes A_j, Q_{1j}, Q_{2j}, Q_{3j} and D_{2j} enter into the same immune class I (this is the tenth class, but common to both subpopulations).

The natural history of new coronavirus infection is the same for young ($j = y$) and elder ($j = o$) subpopulations. We assume that persons in the asymptomatic (A_j), pre-diseased (D_{1j}), and a fraction z_j of non-hospitalized CoViD-19 (Q_{2j}) classes are transmitting the virus, and other infected classes (Q_{1j}, $(1 - z_j)\, Q_{2j}$ and D_{2j}) are under voluntary or forced isolation. Susceptible persons are infected according to $\lambda_j S_j$ (known as mass action law [4]) and enter into class E_j, where λ_j is the per-capita incidence rate (or force of infection) defined by $\lambda_j = \lambda\,(\delta_{jy} + \psi\delta_{jo})$, with λ being

$$\lambda = \frac{1}{N}\left(\varepsilon_{1y}\beta_{1y}A_y + \varepsilon_{2y}\beta_{2y}D_{1y} + \varepsilon_{3y}\beta_{3y}z_yQ_{2y} + \varepsilon_{1o}\beta_{1o}A_o + \varepsilon_{2o}\beta_{2o}D_{1o} + \varepsilon_{3o}\beta_{3o}z_oQ_{2o}\right), \qquad (1)$$

where δ_{ij} is Kronecker delta, with $\delta_{ij} = 1$ if $i = j$, and 0, if $i \neq j$; and β_{1j}, β_{2j} and β_{3j} are the transmission rates, that is, the rates at which a virus encounters a susceptible people and infects, and ε_{1j}, ε_{2j} and ε_{3j} are reduction factors due to protection behaviors. After an average period $1/\sigma_j$ in class E_j, where σ_j is the incubation rate, exposed persons enter into the asymptomatic A_j (with probability p_j) or pre-diseased D_{1j} (with probability $1 - p_j$) classes. After an average period $1/\gamma_j$ in class A_j, where γ_j is the recovery rate of asymptomatic persons, symptomatic persons acquire immunity (recovered) and enter into immune class I. Possibly asymptomatic persons can manifest symptoms at the end of this period, and a fraction $1 - \chi_j$ enter into non-hospitalized Q_{2j} class. Another route of exit from class A_j is being caught by a test at a rate η_j and enter into class I (we assume that this person indeed adopt isolation, which is reason to enter to class I at a rate of testing). With respect to symptomatic persons, after an average period $1/\gamma_{1j}$ in class D_{1j}, where γ_{1j} is the infection rate of pre-diseased persons, pre-diseased persons enter into hospitalized D_{2j} (with probability $1 - m_j$) or non-hospitalized Q_{2j} (with probability m_j) class, or they are caught by test at a rate η_{1j} and enter into class Q_{1j}. Hospitalized persons acquire immunity after a period $1/\gamma_{2j}$, where γ_{2j} is the recovery rate of severe CoViD-19, and enter into immune class I or die under the disease induced (additional) mortality rate α_j. Another route of exiting D_{2j} is by treatment, described by the treatment

rate θ_j. Class Q_{1j} are composed by mild and severe CoViD-19 persons who came from D_{1j} caught by test, hence they enter into hospitalized D_{2j} (with rate $(1-m_j)\,\gamma_{1j}$) or immune I (with rate $m_j\gamma_{1j}+\gamma_{2j}$, assuming adherence to isolation) class. Non-hospitalized Q_{2j} persons acquire immunity after a period $1/\gamma_{3j}$, where γ_{3j} is the recovery rate of mild CoViD-19, and enter into immune class I. Another routes of exit from class Q_{2j} are being caught by a test at a rate η_{2j} and enter into class I (assumption of adherence to isolation), or enter to class Q_{3y} convinced by education campaign at a rate ε_{4j}, which is temporary, hence ξ_j is the rate of abandonment of protection behavior [31].

In the model, we consider pulse isolation and intermittent (series of pulses) release of persons. We assume that there is a unique pulse in isolation at time $t=\tau_j^{is}$, described by $k_jS_j\delta\left(t-\tau_j^{is}\right)$, but there are m intermittent releases described by $\sum_{i=1}^{m} l_{ij}Q_j\delta\left(t-t_i\right)$, where $t_i=\tau_j^{is}+\sum_{w=1}^{i}\tau_{wj}$, $j=y,o$, and $\delta\left(x\right)$ is Dirac delta function, that is, $\delta\left(x\right)=\infty$, if $x=0$, otherwise, $\delta\left(x\right)=0$, with $\int_0^\infty \delta\left(x\right)dx=1$. The parameters k_j is the fraction of persons in isolation, and l_{ij}, $i=1,2,\cdots,m$, is the fractions of i-th release of isolated persons, and τ_{wj} is the period between successive releases.

Figure 1 shows the flowchart of the new coronavirus transmission model.

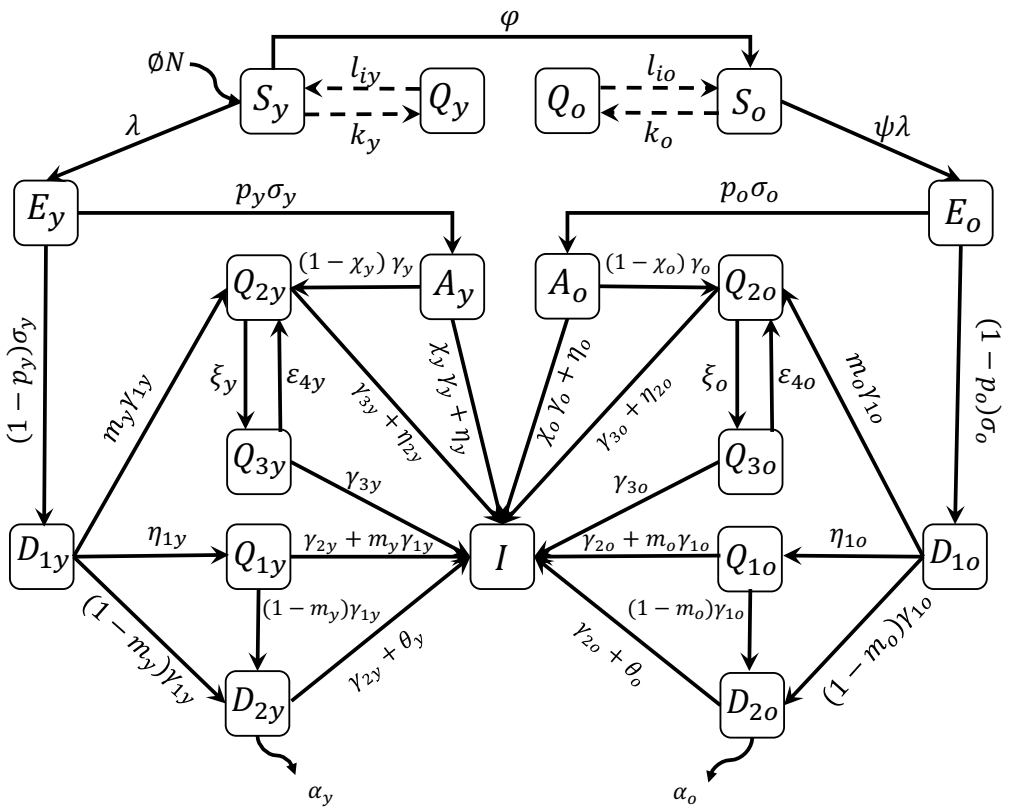

Figure 1: The flowchart of new coronavirus transmission model with variables and parameters.

The new coronavirus transmission model, based on above descriptions summarized in Figure 1, is described by system of ordinary differential equations, with $j=y,o$. Equations for

susceptible persons are

$$\begin{cases} \frac{d}{dt}S_y &= \phi N - (\varphi+\mu)\,S_y - \lambda S_y - k_y S \delta\left(t-\tau_y^{is}\right) + \sum_{i=1}^{m} l_{iy} Q_y \delta\left(t-\tau_j^{is} - \sum_{w=1}^{i}\tau_{wy}\right) \\ \frac{d}{dt}S_o &= \varphi S_y - \mu S_o - \lambda\psi S_o - k_o S_o \delta\left(t-\tau_o^{is}\right) + \sum_{i=1}^{m} l_{io} Q_o \delta\left(t-\tau_j^{is} - \sum_{w=1}^{i}\tau_{wo}\right), \end{cases} \tag{2}$$

for infectious persons,

$$\begin{cases} \frac{d}{dt}Q_j &= k_j S_j \delta\left(t-\tau_j^{is}\right) - \mu Q_j - \sum_{i=1}^{m} l_{ij} Q_j \delta\left(t-\tau_j^{is} - \sum_{w=1}^{i}\tau_{wj}\right) \\ \frac{d}{dt}E_j &= \lambda\left(\delta_{jy}+\psi\delta_{jo}\right) S_j - \left(\sigma_j+\mu\right) E_j \\ \frac{d}{dt}A_j &= p_j\sigma_j E_j - \left(\gamma_j+\eta_j+\mu\right) A_j \\ \frac{d}{dt}D_{1j} &= \left(1-p_j\right)\sigma_j E_j - \left(\gamma_{1j}+\eta_{1j}+\mu\right) D_{1j} \\ \frac{d}{dt}Q_{2j} &= \left(1-\chi_j\right)\gamma_j A_j + m_j\gamma_{1j} D_{1j} + \xi_j Q_{3j} - \left(\gamma_{3j}+\eta_{2j}+\varepsilon_{4j}+\mu\right) Q_{2j} \\ \frac{d}{dt}Q_{3j} &= \varepsilon_{4j} Q_{2j} - \left(\gamma_{3j}+\xi_j+\mu\right) Q_{3j} \\ \frac{d}{dt}Q_{1j} &= \eta_{1j} D_{1j} - \left(\gamma_{2j}+\gamma_{1j}+\mu\right) Q_{1j} \\ \frac{d}{dt}D_{2j} &= \left(1-m_j\right)\gamma_{1j}\left(D_{1j}+Q_{1j}\right) - \left(\gamma_{2j}+\theta_j+\mu+\alpha_j\right) D_{2j}, \end{cases} \tag{3}$$

and for immune persons,

$$\begin{aligned} \frac{d}{dt}I &= \left(\chi_y\gamma_y+\eta_y\right) A_y + \left(\gamma_{2y}+m_y\gamma_{1y}\right) Q_{1y} + \left(\gamma_{3y}+\eta_{2y}\right) Q_{2y} + \gamma_{3y} Q_{3y} + \left(\gamma_{2y}+\theta_y\right) D_{2y} + \\ &\quad \left(\chi_o\gamma_o+\eta_o\right) A_o + \left(\gamma_{2o}+m_o\gamma_{1o}\right) Q_{1o} + \left(\gamma_{3o}+\eta_{2o}\right) Q_{2o} + \gamma_{3o} Q_{3o} + \left(\gamma_{2o}+\theta_o\right) D_{2o} - \mu I, \end{aligned} \tag{4}$$

where $N_j = S_j + Q_j + E_j + A_j + D_{1j} + Q_{1j} + Q_{2j} + Q_{3j} + D_{2j}$, and $N = N_y + N_o + I$ obeys

$$\frac{d}{dt}N = \left(\phi-\mu\right) N - \alpha_y D_{2y} - \alpha_o D_{2o}, \tag{5}$$

with the initial number of population at $t=0$ being $N(0) = N_0 = N_{0y} + N_{0o}$, where N_{0y} and N_{0o} are the number of young and elder persons at $t=0$. If $\phi = \mu + \left(\alpha_y D_{2y} + \alpha_o D_{2o}\right)/N$, the total size of the population is constant.

Table 1 summarizes the model variables (or classes).

The non-autonomous system of equations (2), (3), and (4) is simulated letting intermittent interventions to the boundary conditions. Hence, the equations for susceptible and isolated persons become

$$\begin{cases} \frac{d}{dt}S_y &= \phi N - \left(\varphi+\mu\right) S_y - \lambda S_y \\ \frac{d}{dt}S_o &= \varphi S_y - \mu S_o - \lambda\psi S_o \\ \frac{d}{dt}Q_y &= -\mu Q_j, \end{cases} \tag{6}$$

Table 1: Summary of the model variables ($j = y, o$).

Symbol	Meaning
S_j	Susceptible persons
Q_j	Isolated among susceptible persons
E_j	Exposed and incubating new coronavirus persons
A_j	Asymptomatic persons
D_{1j}	Pre-diseased (pre-symptomatic) persons
Q_{1j}	Pre-diseased persons caught by test
Q_{2j}	Mild (non-hospitalized) CiViD-19 persons
Q_{3j}	Mild CiViD-19 persons adhered to isolation
D_{2j}	Severe (hospitalized) CoViD-19 persons
I	Immune (recovered) persons

$j = y, o$, and other equations are the same.

For the system of equations (6), (3), and (4), the initial conditions (at $t = 0$) are, for $j = y, o$,

$$S_j(0) = N_{0j}, \quad X_j(0) = n_{X_j}, \quad \text{where} \quad X_j = Q_j, E_j, A_j, D_{1j}, Q_{1j}, Q_{2j}, Q_{3j}, D_{2j}, I, \tag{7}$$

and n_{X_j} is a non-negative number. For instance, $n_{E_y} = n_{E_o} = 0$ means that there is not any exposed individual (young and elder) at the beginning of epidemics. We split the boundary conditions into isolation and release, and assume that $\tau^{is} = \tau_y^{is} = \tau_o^{is}$ and $\tau_i = \tau_{iy} = \tau_{io}$, for $i = 1, 2, \cdots, m$, then $t_i = \tau^{is} + \sum_{w=1}^{i} \tau_w$. A unique isolation at $t = \tau^{is}$ is described by the boundary conditions

$$S_j(\tau^{is+}) = S_j(\tau^{is-})(1 - k_j) \quad \text{and} \quad Q_j(\tau^{is+}) = Q_j(\tau^{is-}) + S_j(\tau^{is-})\, k_j \tag{8}$$

plus

$$X_j(\tau^{is+}) = X_j(\tau^{is-}), \quad \text{where} \quad X_j = E_j, A_j, D_{1j}, Q_{1j}, Q_{2j}, Q_{3j}, D_{2j}, I. \tag{9}$$

where we have $\tau^{is-} = \lim_{t \to \tau^{is}} t$ (for $t < \tau^{is}$), and $\tau^{is+} = \lim_{\tau^{is} \leftarrow t} t$ (for $t > \tau^{is}$). The boundary conditions for a series of pulses released at $t_i = \tau^{is} + \sum_{w=1}^{i} \tau_w$, for $i = 1, 2, \cdots, m$, are

$$S_j(t_i^+) = S_j(t_i^-) + l_{ij} Q_j(t_i^-) \quad \text{and} \quad Q_j(t_t^+) = (1 - l_{ij})\, Q_j(t_i^-), \tag{10}$$

plus

$$X_j(t_i^+) = X_j(t_i^-), \quad \text{where} \quad X_j = E_j, A_j, D_{1j}, Q_{1j}, Q_{2j}, Q_{3j}, D_{2j}, I. \tag{11}$$

If $\tau = \tau_i$, then $t_i = \tau^{is} + i\tau$. If isolation is applied to a completely susceptible population, at $t = 0$, there are not any infectious person, so $S(0) = N_0$. If isolation is done at $t = \tau_j^{is}$ without screening of persons harboring the virus, then many of them could be isolated with susceptible persons.

Table 2 summarizes the model parameters and values (for elder classes, values are between parentheses).

From the system of equations (2), (3), and (4) we can derive some epidemiological parameters: new hospitalized CoViD-19 cases, number of occupied beds by inpatient, ICU and

Table 2: Summary of the model parameters ($j = y, o$) and values (rates in $days^{-1}$, time in $days$ and proportions are dimensionless). Some values are calculated ($^{\#}$), or assumed (*), or estimated (**) or not available yet (***).

Symbol	Meaning	Value
μ	Natural mortality rate	$1/(75 \times 360)$[14]
ϕ	Birth rate	$1/(75 \times 360)^{*}$
φ	Aging rate	$6.7 \times 10^{-6\#}$
$\sigma_y\,(\sigma_o)$	Incubation rate	$1/5.8\,(1/5.8)^{\#}$
$\gamma_y\,(\gamma_o)$	Recovery rate of asymptomatic persons	$1/12\,(1/14)$[18]
$\gamma_{1y}\,(\gamma_{1o})$	Infection rate of pre-diseased persons	$1/4\,(1/4)$[2]
$\gamma_{2y}\,(\gamma_{2o})$	Recovery rate of severe CoViD-19	$1/14\,(1/21)$[18]
$\gamma_{3y}\,(\gamma_{3o})$	Infection rate of mild CoViD-19 persons	$1/13\,(1/16)^{*}$
$\alpha_y\,(\alpha_o)$	Additional mortality rate	$0.00053\,(0.0053)^{**}$
$\eta_y\,(\eta_o)$	Testing rate among asymptomatic persons	$0\,(0)^{***}$
$\eta_{1y}\,(\eta_{1o})$	Testing rate among pre-diseased persons	$0\,(0)^{***}$
$\eta_{2y}\,(\eta_{2o})$	Testing rate among mild CoViD-19 persons	$0\,(0)^{***}$
$\varepsilon_{4y}\,(\varepsilon_{4o})$	Adherence to protection behavior rate	$0.5\,(0.5)^{**}$
$\xi_y\,(\xi_o)$	Loss of protection behavior rate	$0\,(0)^{***}$
$k_y\,(k_o)$	Proportion of isolated susceptible persons	$0.528\,(0.528)^{**}$
$l_{1y}\,(l_{1o})$	Proportion released at first time t_1	$0.33\,(0.33)^{*}$
τ^{is}	Time of the introduction of isolation	March 24
$\tau_{1y}(\tau_{1o})$	Time of the first (i-th) releasing	June 1(June 1)*
$\theta_y\,(\theta_o)$	Treatment rate	$0(0)^{***}$
$\beta_{1y}\,(\beta_{1o})$	Transmission rate due to asymptomatic persons	$0.81\,(0.932)^{**}$
$\beta_{2y}\,(\beta_{2o})$	Transmission rate due to pre-diseased persons	$0.81\,(0.932)^{**}$
$\beta_{2y}\,(\beta_{2o})$	Transmission rate due to mild CoViD-19 persons	$0.81\,(0.932)^{**}$
$z_y\,(z_o)$	Proportion circulating of mild CoViD-19 persons	$0.5\,(0.2)^{*}$
ψ	Scaling factor of transmission among elder persons	1.15^{**}
$\chi_y\,(\chi_o)$	Proportion of remaining as asymptomatic persons	$0.98\,(0.95)^{***}$
$p_y\,(p_o)$	Proportion of asymptomatic persons	$0.8(0.8)^{*}$
$m_y\,(m_o)$	Proportion of mild (non-hospitalized) CoViD-19	$0.92^{\#}$ (0.75[6])

ICU/intubated persons, the number of cured persons, and number of deaths due to CoViD-19. All initial conditions below are determined by the initial conditions (7) supplied to the system of equations.

The number of circulating and in isolation susceptible persons is obtained from

$$S^{tot} = S_y^{tot} + S_o^{tot}, \qquad \text{where} \qquad \begin{cases} S_y^{tot} = S_y + Q_y \\ S_o^{tot} = S_o + Q_o, \end{cases} \tag{12}$$

where S_y^{tot} and S_o^{tot} are the potential numbers of susceptible, respectively, young and elder persons to be infected.

The numbers of new hospitalized CoViD-19 cases Ω_y and Ω_o are given by exits from D_{1y},

Q_{1y}, D_{1o}, and Q_{1o}, and entering into classes D_{2y} and D_{2o}, that is,

$$\Omega = \Omega_y + \Omega_o, \quad \text{with} \quad \begin{cases} \dfrac{d}{dt}\Omega_y = (1-m_y)\,\gamma_{1y}\,(D_{1y}+Q_{1y}) \\ \dfrac{d}{dt}\Omega_o = (1-m_o)\,\gamma_{1o}\,(D_{1o}+Q_{1o}) \end{cases} \tag{13}$$

with $\Omega_y(0) = \Omega_{y0}$ and $\Omega_o(0) = \Omega_{o0}$. The number of deaths due to severe CoViD-19 is

$$\Pi = \Pi_y + \Pi_o, \quad \text{where} \quad \begin{cases} \dfrac{d}{dt}\Pi_y = \alpha_y D_{2y}, \quad \text{with} \quad \Pi_y(0) = 0 \\ \dfrac{d}{dt}\Pi_o = \alpha_o B_{1o}, \quad \text{with} \quad \Pi_o(0) = 0. \end{cases} \tag{14}$$

These two variables are used to estimate model parameters.

The daily new hospitalized CoViD-19 cases Ω_d is, considering $\Delta t = t_i - t_{i-1} = \Delta t = 1\ day$,

$$\Omega_d(t_i) = \int_{t_{i-1}}^{t_i} \tfrac{d}{dt}\Omega dt = \Omega\,(t_i) - \Omega\,(t_{i-1})\,, \tag{15}$$

where $\Omega_d(0) = \Omega_{d0}$ is the first observed CoViD-19 cases ($t_0 = 0$), with $i = 1, 2, \cdots$, and $t_1 = 1$ is the next day in the calendar time, and so on.

The number of beds occupied by inpatients during the evolving of epidemics is $B_1 = B_{1y} + B_{1o}$, for $j = y, o$, where

$$\begin{cases} \dfrac{d}{dt}B_{1y} = h_y \dfrac{d}{dt}\Omega_y - (\mu + \varsigma_{1y})\,B_{1y}, \quad \text{with} \quad B_{1y}(0) = B_{1y0} \\ \dfrac{d}{dt}B_{1o} = h_o \dfrac{d}{dt}\Omega_o - (\mu + \varsigma_{1o})\,B_{1o}, \quad \text{with} \quad B_{1o}(0) = B_{1o0}, \end{cases} \tag{16}$$

number of beds occupied by ICU persons is $B_2 = B_{2y} + B_{2o}$, where

$$\begin{cases} \dfrac{d}{dt}B_{2y} = h_{1y}\varsigma_{1y}B_{1y} - (\mu + \varsigma_{2y})\,B_{2y}, \quad \text{with} \quad B_{2y}(0) = B_{2y0} \\ \dfrac{d}{dt}B_{2o} = h_{1o}\varsigma_{1o}B_{1o} - (\mu + \varsigma_{2o})\,B_{2o}, \quad \text{with} \quad B_{2o}(0) = B_{2o0}, \end{cases} \tag{17}$$

and number of beds occupied by ICU/intubated persons is $B_3 = B_{3y} + B_{3o}$, where

$$\begin{cases} \dfrac{d}{dt}B_{3y} = h_{2y}\varsigma_{2y}B_{2y} - (\mu + \varsigma_{3y})\,B_{3y}, \quad \text{with} \quad B_{3y}(0) = B_{3y0} \\ \dfrac{d}{dt}B_{3o} = h_{2o}\varsigma_{2o}B_{2o} - (\mu + \varsigma_{3o})\,B_{3o}, \quad \text{with} \quad B_{3o}(0) = B_{3o0}. \end{cases} \tag{18}$$

We assumed that a proportion h_j of all severe CiViD-19 patients are hospitalized and enter into class of bed B_1, from which a proportion h_{1j} needs ICU care (class of bed B_2), and among them a proportion h_{2j} needs ICU/intubating care (class of bed B_3). The average occupying time of beds by inpatient, ICU and ICU/intubated persons are, respectively, $1/\varsigma_{1j}$, $1/\varsigma_{2j}$ and $1/\varsigma_{3j}$, where ς_{1j}, ς_{2j} and ς_{3j} are the discharging rates from hospital, ICU and ICU/intubating care; and α_{1j} and α_{2j} are the additional mortality (fatality) proportions among inpatient, ICU

and ICU/intubating persons, for $j = y, o$. The fraction $1 - h_{1j}$ is possibly non-hospitalization (short-time in hospital care) of severe CoViD-19; and $1-h_{1j}-\alpha_{1j}$, $1-h_{2j}-\alpha_{2j}$ and $1-h_{3j}$ are the proportions of cure of inpatient, ICU and ICU/intubated persons, where α_{3j} is the proportion dying in ICU/intubated class. The total number of occupied beds is $B = B_1 + B_2 + B_3$.

The total number of persons being cured is $C = C_y + C_o$ where

$$\begin{cases} \dfrac{d}{dt}C_y = (1 - h_{1y} - \alpha_{1y})\,\varsigma_{1y}B_{1y} + (1 - h_{2y} - \alpha_{2y})\,\varsigma_{2y}B_{2y} + (1 - \alpha_{3y})\,\varsigma_{3y}B_{3y} - \mu C_y, & \text{with} \quad C_y(0) = 0 \\ \dfrac{d}{dt}C_o = (1 - h_{1o} - \alpha_{1o})\,\varsigma_{1o}B_{1o} + (1 - h_{2o} - \alpha_{2o})\,\varsigma_{2o}B_{2o} + (1 - \alpha_{3o})\,\varsigma_{3o}B_{3o} - \mu C_o, & \text{with} \quad C_o(0) = 0. \end{cases} \tag{19}$$

The number of deaths caused by severe CoViD-19 cases can be calculated from hospitalized cases. The number of deaths for inpatients is $\Pi_1 = \Pi_{1y} + \Pi_{1o}$, where

$$\begin{cases} \dfrac{d}{dt}\Pi_{1y} = \alpha_{1y}\varsigma_{1y}B_{1y}, & \text{with} \quad \Pi_{1y}(0) = 0 \\ \dfrac{d}{dt}\Pi_{1o} = \alpha_{1o}\varsigma_{1o}B_{1o}, & \text{with} \quad \Pi_{1o}(0) = 0, \end{cases} \tag{20}$$

the number for ICU care persons is $\Pi_2 = \Pi_{2y} + \Pi_{2o}$, where

$$\begin{cases} \dfrac{d}{dt}\Pi_{2y} = \alpha_{2y}\varsigma_{2y}B_{2y}, & \text{with} \quad \Pi_{2y}(0) = 0 \\ \dfrac{d}{dt}\Pi_{2o} = \alpha_{2o}\varsigma_{2o}B_{2o}, & \text{with} \quad \Pi_{2o}(0) = 0, \end{cases} \tag{21}$$

and the number for ICU/intubated persons is $\Pi_3 = \Pi_{3y} + \Pi_{3o}$, where

$$\begin{cases} \dfrac{d}{dt}\Pi_{3y} = \alpha_{3y}\varsigma_{3y}B_{3y}, & \text{with} \quad \Pi_{3y}(0) = 0 \\ \dfrac{d}{dt}\Pi_{3o} = \alpha_{3o}\varsigma_{3o}B_{3o}, & \text{with} \quad \Pi_{3o}(0) = 0. \end{cases} \tag{22}$$

Table 3 summarizes parameters related to hospitalization and values (for elder classes, values are between parentheses).

The system of equations (2), (3), and (4) is non-autonomous. Nevertheless, the fractions of persons in each compartment approach the steady state (see Appendix A). Hence, at $t = 0$, the basic reproduction number R_0 is obtained substituting s_y^0 and s_o^0 by N_{0y}/N_0 and N_{0o}/N_0 in equation (A.4), resulting in

$$R_0 = R_y\frac{N_{0y}}{N_0} + R_o\frac{N_{0o}}{N_0} = (R_{1y} + R_{2y})\,\frac{N_{0y}}{N_0} + (R_{1o} + R_{2o})\,\frac{N_{0o}}{N_0}, \tag{23}$$

and using equations (A.9) and (A.8).

Let us use the approximated effective reproduction number R_{ef} given by equation (A.11), that is,

$$R_{ef} = (R_{1y} + R_{2y})\,\frac{S_y}{N} + (R_{1o} + R_{2o})\,\frac{S_o}{N}, \tag{24}$$

Table 3: Summary of the parameters related to hospitalization ($j = y, o$) and values (rates in $days^{-1}$ and proportions are dimensionless). Some values are assumed (*) or estimated (**).

Symbol	Meaning	Value
$\alpha_{1y}\,(\alpha_{1o})$	Fatality proportion of inpatients	$0.01(0.05)^{**}$
$\alpha_{2y}\,(\alpha_{2o})$	Fatality proportion of persons in ICU	$0.05(0.15)^{**}$
$\alpha_{3y}\,(\alpha_{3o})$	Fatality proportion of persons in ICU/intubated	$0.15(0.35)^{**}$
$\varsigma_{1y}\,(\varsigma_{1o})$	Discharge rate of inpatients from hospital	$1/5(1/6)^{*}$
$\varsigma_{2y}\,(\varsigma_{2o})$	Discharge rate from ICU	$1/7\,(1/8)^{*}$
$\varsigma_{3y}\,(\varsigma_{3o})$	Discharge rate from ICU/intubated	$1/15\,(1/20)^{*}$
$h_y\,(h_o)$	Proportion needing long-stay in hospital	$1.0\,(1.0)^{*}$
$h_{1y}\,(h_{1o})$	Proportion needing ICU	$0.15\,(0.25)^{**}$
$h_{2y}\,(h_{2o})$	Proportion of ICU needing ICU/intubated	$0.2(0.4)^{**}$

where R_y and R_o are given by equation (A.9). For $t > 0$, we have the effective reproduction number R_{ef}, with $R_{ef}(0) = R_0$ at $t = 0$, which decreases as susceptible persons decrease. However, at $t = \tau^{is}$ a pulse in isolation is introduced, hence we have $R_{ef}(\tau^{is+}) = R_r$, where the reduced reproduction number R_r is given by

$$R_r = (R_{1y} + R_{2y})\,\frac{S_y\left(\tau^{is-}\right)(1-k_y)}{N_0} + (R_{1o} + R_{2o})\,\frac{S_o\left(\tau^{is-}\right)(1-k_o)}{N_0}, \tag{25}$$

where $S_y\left(\tau^{is-}\right)$ and $S_o\left(\tau^{is-}\right)$ are the numbers of susceptible young and elder persons at the time just before the introduction of isolation. Notice that at $t = \tau^{is}$, $R_{ef}(\tau^{is-})$ jumped down to $R_{ef}(\tau^{is+})$. At i-th release time t_i, we have $R_{ef}(t_i^+) = R_u(i)$, with the up (increased) reproduction number $R_u(i)$ being given by

$$R_u(i) = (R_{1y} + R_{2y})\,\frac{S_y\left(t_i^-\right) + l_{iy}Q_y\left(t_i^-\right)}{N_0} + (R_{1o} + R_{2o})\,\frac{S_o\left(t_i^-\right) + l_{io}Q_o\left(t_i^-\right)}{N_0}, \tag{26}$$

where $R_{ef}(t_i^-)$ jumped up to $R_{ef}(t_i^+)$ at $t = t_i$. After $t > t_m$, there is not release anymore, and $R_{ef} = 1$ when $t \to \infty$, and the new coronavirus returns to the original dynamics driven by R_0.

Given N and R_0, let us evaluate the size of population to trigger and maintain epidemics. Letting $R_{ef} = 1$ and assuming that $R_y = R_o$, the critical size of population N^{th} is

$$N^{th} \approx \frac{N}{R_0}. \tag{27}$$

If $N > N^{th}$, epidemics occurs and persists ($R_0 > 1$, and epidemics is driven toward the non-trivial equilibrium point P^*), and the fraction of susceptible individuals is $s^* = 1/R_0$, where $s^* = s_y^* + s_o^*$; but if $N < N^{th}$, epidemics occurs but fades out ($R_0 < 1$, and epidemics is driven toward the trivial equilibrium point P^0), and the fractions of susceptible individuals s_y and s_o at equilibrium are given by equation (A.4).

We apply the above results to study the introduction and spreading of the new coronavirus in São Paulo State, Brazil.

3 Results

The results obtained in the foregoing section are applied to describe the new coronavirus infections in São Paulo State, Brazil. The first confirmed case of CoViD-19, occurred on February 26, 2020, was a traveler returning from Italy on February 21, and being hospitalized on February 24. The first death due to CoViD-19 was a 62 years old male with comorbidity who never travelled to abroad, hence considered as autochthonous transmission. He manifested the first symptoms on March 10, was hospitalized on March 14, and died on March 16. On March 24, the São Paulo State authorities ordered isolation of persons acting in non-essential activities, as well as students of all levels until April 6, further isolation was extended to April 22, and postponed first to May 10 and then, 31.

The dynamics of the new coronavirus propagation is obtained by evaluating the system of equations (2), (3), and (4) numerically using the 4^{th} order Runge-Kutta method. Let us determine the initial conditions supplied to this system. In São Paulo State, the number of inhabitants is $N(0) = N_0 = 44.6 \times 10^6$ [14]. The value of parameter φ given in Table 1 was calculated by rewriting the equation (A.4) as $\varphi = b\phi/(1-b)$, where b is the proportion of elder persons. Using $b = 0.153$ in São Paulo State [14], we obtained $\varphi = 6.7 \times 10^{-6}\ days^{-1}$, hence, $N_y(0) = N_{0y} = 37.8 \times 10^6$ ($s_y^0 = N_{0y}/N_0 = 0.8475$) and $N_o(0) = N_{0o} = 6.8 \times 10^6$ ($s_o^0 = N_{0o}/N_0 = 0.1525$). The initial conditions for susceptible persons are set to be $S_y(0) = N_{0y}$ and $S_o(0) = N_{0o}$.

The initial conditions for other variables are calculated based on Table 2. Using $p_y = p_o = 0.8$, the ratio asymptomatic:symptomatic is $4:1$ for young and elder persons; using $m_o = 0.75$, the ratio mild:severe (or non-hospitalized:hospitalized) CoViD-19 is $3:1$ for elder persons, and for young persons, ratio is $12:1$ from $m_y = 0.92$. Hence, for elder subpopulation, if we assume that there is one person in D_{2o} (the first confirmed case), then there are 3 persons in Q_{2o}; the sum (4) is the number of persons in class D_{1o}, implying that there are 16 in class A_o, hence, the sum (20) is the number of persons in class E_o. Notice that, if there is 1 person in D_{2y}, then there must be 12 persons in Q_{2y}. For young subpopulation, we assume that there is not any person in D_{2y}, but 6 persons in Q_{2y}, then the sum (6) is the number of persons in class D_{1y}, implying that there are 24 in class A_y, hence, the sum (30) is the number of persons in class E_y. Finally, we suppose that no one is isolated or tested, and immunized. (Probably the first confirmed COViD-19 person transmitted virus (since February 21 when returned infected from Italy), as well as other asymptomatic travelers returning from abroad.)

Therefore, the initial conditions supplied to the dynamic system (2), (3), and (4) are, for elder subpopulation,

$$\begin{cases} S_o(0) = N_{0o}, \quad Q_o(0) = Q_{1o}(0) = Q_{3o}(0) = 0, \quad E_o(0) = 20, \\ A_o(0) = 16, \quad D_{1o}(0) = 4, \quad Q_{2o}(0) = 3 \quad D_{2o}(0) = 1, \quad I(0) = 0, \end{cases}$$

and for young subpopulation,

$$\begin{cases} S_y(0) = N_{0y}, \quad Q_y(0) = Q_{1y}(0) = Q_{3y}(0) = 0, \quad E_y(0) = 30, \\ A_y(0) = 24, \quad D_{1y}(0) = 6, \quad Q_{2y}(0) = 6 \quad D_{2y}(0) = 0, \quad I(0) = 0, \end{cases}$$

where the initial simulation time $t = 0$ corresponds to the calendar time February 26, 2020, when the first case was confirmed.

This section presents parameters estimation and epidemiological scenarios considering isolation as the control mechanism. In these scenarios, we assume that all transmission rates in young persons are equal, as well as in elder persons, that is, we assume that

$$\beta_y = \beta_{1y} = \beta_{2y} = \beta_{3y} = \beta_{1o} = \beta_{2o} = \beta_{3o}, \qquad \text{and} \qquad \beta_o = \psi\beta_y,$$

hence, the forces of infection are $\lambda_y = (A_y + D_{1y} + z_y Q_{2y} + A_o + D_{1o} + z_o Q_{2o})\,\beta_y/N$ and $\lambda_o = \psi\lambda_y$, where $\varepsilon_{ij} = 1$, with $i = 1, 2, 3$, and $j = y, o$ (there are not any interventions in the beginning of epidemics). The reason to include factor ψ is the reduced capacity of defense mechanism by elder persons (physical barrier, innate and adaptive immune responses, etc.). The force of infection takes into account all virus released by infectious individuals (A_y, D_{1y}, Q_{2y}, A_o, D_{1o} and Q_{2o}), the rate of encounter with susceptible persons, and the capacity to infect them (see [20] [21]). Additionally, the amount inhaled by susceptible persons can be determinant in the chance of infection and in the prognostic of CoViD-19 [28].

From data collected in São Paulo State from February 26 until May 7, 2020, we fit transmission (β_y and β_o) and fatality (α_y and α_o) rates, the proportions of isolated persons (k_y and k_o), and reduction in the transmission rates due to protection actions adopted by people (ε).[1] Once determined these parameters, we study potential scenarios introducing isolation as control mechanisms and subsequent release.

3.1 Parameters estimation

Reliable estimations of both transmission and additional mortality rates is crucial, aiming to study the emerging of new cases (to an adequate number of beds in hospital, for instance) and deaths. When the estimation is based on a few number of data, that is, at the beginning of epidemics, some cautions must be taken, because the rates maybe over or under estimated. The reason is that in the very beginning phase of epidemic, the spreading of infections and deaths increase very quickly.

Currently, there is not a sufficient number of kits to detect infection by the new coronavirus. For this reason, test to confirm infection by this virus is done only in hospitalized persons, and also in persons who died manifesting symptoms of CoViD-19. Hence, we have only data of new hospitalized persons ($\Omega = \Omega_y + \Omega_o$) and those who died ($\Pi = \Pi_y + \Pi_o$). Taking into account hospitalized persons with CoViD-19, we fit the transmission rates, and for persons died due to CoViD-19, we fit the additional mortality rates. These rates are fitted applying the least square method (see [13]), that is

$$\min \sum_{i=1}^{n} \left[Z\left(t_i\right) - Z^{ob}\left(t_i\right) \right]^2, \tag{28}$$

where min stands for the minimum value, n is the number of observations, t_i is i-th observation time, Z stands for Ω given by equation (13), or Π given by equation (14); and Z^{ob} stands for the observed number of new hospitalized persons Ω^{ob} or number of died persons Π^{ob}. The fitted parameters are those minimizing the sum of squared differences.

[1] Simulations were done on May 7-8.

Figure 2 shows the daily (a) and accumulated (b) CoViD-19 new cases, plus observed proportions in isolation. In Figure 2(a), we moved the proportions in isolation showed in Figure 2(b) 9 days forward (for instance, the number of cases registered on April 10 corresponds to proportion inn isolation observed on April 1). The horizontal line in Figure 2(a) corresponds to the mean value $k_{mean} = 0.528$, around which daily proportions vary impacting on the transmission. We use the observed proportions of isolated persons [1] and new hospitalized CoViD-19 cases [3] in São Paulo State from March 24 to May 7.

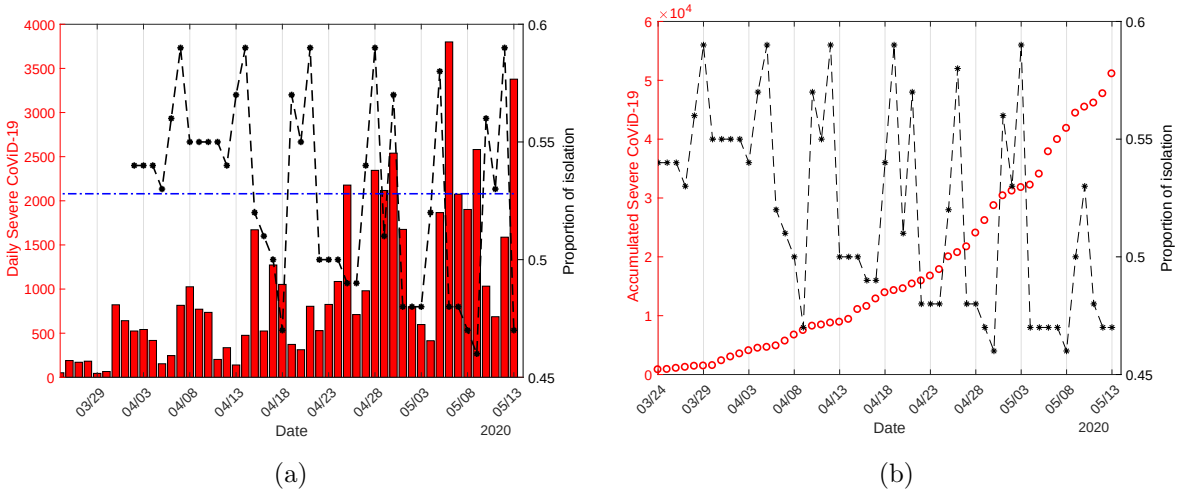

(a) (b)

Figure 2: Figure 2 shows the daily (a) and accumulated (b) CoViD-19 cases collected from March 24 to May 3 [3], plus observed proportion in isolation moved 9 days forward.

We discuss the collected data roughly (observing the trend of data, but not scientifically based). Interestingly, Figure 2(a) shows that the daily data present weekly seasonality, with lower cases at the weekend [3], due maybe to registering the day at which occurred the confirmation by laboratory testing, not the beginning of symptoms.

(A) The number of SARS in São Paulo State registered in the site of Ministry of Health (Brazil) [10] shows increasing beyond the average cases occurred in past years since March 8, 2020 (around $1,000$ cases in the 11^{th} epidemiological week (hereafter, week), March 8-14), and reach peak 2 weeks later (around $4,000$ cases in the 13^{th} week, March 22-28). After this epidemiological week, the notification as SARS initiates decreasing trend, maybe due to increased testing of severe CoViD-19 cases (on March 31, there were 822 cases, but one day earlier, only 66 cases, and around 180 cases a day in the 13^{th} week). Figure 2(b) shows this jump up on March 31. This increased number of cases should be explained by more testing among SARS to identify CoViD-19, or by the exponential-like increasing of epidemics in the beginning, or probably by both. Figure 2(a) shows an unusual jump up when comparing 13^{th} week (March 22-28) and 14^{th} week (March 29-April 4), which is not observed in next weeks, suggesting that the isolation decreased the force of dynamics. Indeed, the isolation was introduced on March 24, but after 10 days, on April 3, there is a change in the exponential-like trend, becoming less abrupt. Figure 2(b) shows increasing trend in blocks of week affected by weekly seasonality shown in Figure 2(a) depending on the proportion in isolation occurred 9 or 10 days earlier. In

a future work, we deal with the depending of the accumulated cases with proportion in isolation delayed in $\Delta = 9$ days, that is, $\Omega(t + \Delta) = \Omega(t, k(t + \Delta))$.

(B) Let us roughly compare severe CoViD-19 cases and isolation week by week. Notice that there is a jump up from the 13^{th} to 14^{th} week, showing exponential-like increase. However, there is not jump to the 15^{th} week (April 5-11), possibly showing the effects of isolation. In the next 16^{th} week (April 12-18) there was strong variations in the CoViD-19 cases, maybe due to huge variation in the proportions in isolation 9 days earlier. In the 17^{th} week (April 19-25), the increased number of cases corresponds to decreased proportions in isolation including weekend (on April 25, Sunday, there was the highest number of cases). This increased trend continued on the next 18^{th} week (April 26-May 2), when the proportions in isolation fluctuated, but relatively small number of cases was registered during the extended holiday (May 1-3). The behavior observed in the 17^{th} and 18^{th} weeks may be the effects of manifestation against isolation occurred on April 18: The peak on April 25 and high number of cases lasting until April 30, that is, 7 to 12 days after the manifestation is the interval with median 9.5 and variation 2.5 (sum of incubation and pre-diseased periods is 9.8). Should this behavior be the prolonged effect of one day crowding?

With respect to parameter values, the transmission and fatality rates, proportion of isolated persons, and reduction in the transmission are estimated. Some values are found in literature, other parameters are calculated or reasonable values are assigned. For incubation period, we use mean value between 5.2 [12] and 6.4 [5], that is, $\sigma = \sigma_y = \sigma_o = 1/5.8\ days^{-1}$. We use for the infectious rates of pre-diseased persons, $\gamma_1 = \gamma_{1y} = \gamma_{1o} = 1/4\ days^{-1}$ [2], and also due to delay observed in 9 days between low isolation and increase in CoViD-19 cases (see below, Figure 2). It was observed approximately 2 weeks for the duration of mild disease, then we use $\gamma_o = 1/14$ and $\gamma_y = 1/12$ (both in $days^{-1}$), and critical disease lasts 2-6 weeks, then we use $\gamma_{2o} = 1/21$ and $\gamma_{2y} = 1/12$ (both in $days^{-1}$) [18].

Let us assume that the ratios between asymptomatic and symptomatic young and elder persons are equal, that is, $p = p_y = p_o = 4/5 = 0.8$ (80.9% of infections are mild and can recover at home [16]). From São Paulo State, 76% of deaths due to CoViD-19 are 60 years old or above, then the ratio of death is $1:3$ to young persons [3]. However, the ratio may be lower in severe CoViD-19 cases, then we assume $2:3$ (in São Bernardo de Campo City, São Paulo State, the ratio of hospitalized young and elder persons is $2:3.3$).[2] We assume that the ratio between asymptomatic and symptomatic among elder persons is $3:1$, hence $m_o = 3/4 = 0.75$. In order to have ratio $2:3$ between young and elder in hospitalized persons, we must have approximately $10:1$ in the ratio between asymptomatic and symptomatic among young persons. We used to calculate approximately

$$c = \frac{1-b}{b} \times \frac{1}{4} \times \frac{2}{3},$$

where the term $(1-b)/b$ is the populational ratio between young and elder persons, $1/4$ is the proportion of severe CoViD-19 cases among elder persons, and $2/3$ is the ratio between hospitalized young and elder persons. Using $b = 0.153$, we have $c = 0.92$. Hence, the ratio asymptomatic:symptomatic among young persons is approximately $12:1$, which results in $m_y = 12/13 = 0.92$, which changes if p_y and p_o are not equal.

[2]Personal communication.

Instead of using equation (28), the least square estimation method, we vary the parameters and choose better fitting by evaluating the sum of squared distances between curve and data.

3.1.1 Fitting the transmission rates

The introduction of isolation was on March 24, but the effects are expected to appear later. Hence, we will estimate taking into account the confirmed cases from February 26 (t_1) to April 5 (t_{40}), totalizing $n = 40$ observations. It is expected that at around April 2 the effects of isolation will appear (the sum of incubation and pre-diseased infection periods (see Table 2) is 9.8 days).

To fit transmission parameters, we can use daily registered new CoViD-19 data (Figure 2(a)) using equation (15), or accumulated new cases (Figure 2(b) using equation (13). However, the accumulated CoViD-19 new cases present less fluctuation, which is the reason to use this collection of data to estimate β_y and β_o. The fatality rates α_y and α_o do not affect on this estimation.

To estimate the transmission rates β_y and β_o, the system of equations (2), (3), and (4), with initial conditions given by equation (7), is evaluated, and we calculate

$$\sum_{i=1}^{n} \left[\Omega\left(t_i\right) - \Omega^{ob}\left(t_i\right)\right]^2$$

by varying β_y and β_o, where the number of accumulated CoViD-19 cases Ω is given by equation (13). We chose the transmission rates minimizing the sum of differences. Letting additional mortality rates equal to zero ($\alpha_y = \alpha_o = 0$), we estimate β_y and $\beta_o = \psi\beta_y$, against new hospitalized CoViD-19 cases ($\Omega = \Omega_y + \Omega_o$) data from the São Paulo State. The estimated values are $\beta_y = 0.78$ and $\beta_o = 0.897$ (both in $days^{-1}$), where $\Psi = 1.15$, resulting in the basic reproduction number $R_0 = 9.239$ (partials $R_{0y} = 7.725$ and $R_{0o} = 1.514$), according to equation (23). Figure 3(a) shows the estimated curve of Ω and observed data, plus two curves with lower transmission rates: $\beta_y = 0.59$ and $\beta_o = 0.679$ (both in $days^{-1}$), with $R_0 = 6.99$ (partials $R_{0y} = 5.84$ and $R_{0o} = 1.16$); and $\beta_y = 0.43$ and $\beta_o = 0.495$ (both in $days^{-1}$), with $R_0 = 5.09$ (partials $R_{0y} = 4.26$ and $R_{0o} = 0.84$). Figure 3(b) shows extended curves of Ω, which approach approach asymptotes (or plateaus), which can be understood as the time when the first wave of epidemics ends. For $R_0 = 9.239$, 6.99 and 5.09, the curves Ω reach values on September 13, respectively, 9.464×10^5, 9.457×10^5, and 9.415×10^5. For $R_0 = 9.239$, the curves for young (Ω_y), elder (Ω_o) and total (Ω) persons approach plateaus (figure not shown) on September 13 with values respectively, 6.053×10^5, 3.411×10^5, and 9.464×10^5.

We pointed out the question of subnotification, nevertheless we use the transmission rates estimated with available data of CoViD-19. We stress the fact that, if the observed data are fitted without cautions about interventions, someone could estimate the basic reproduction number to be $R_0 = 5.09$ or less (near horizontal axis, the observed data seem to approach curve of $R_0 = 5.09$).

The basic reproduction number estimated by our model is $R_0 = 9.239$. However, if we estimate the basic reproduction number using SIR model with different infective persons at $t = 0$, we obtain $R_0 = 3.22$ (for $I(0) = 10$), $R_0 = 2.66$ (for $I(0) = 25$) and $R_0 = 2.38$ (for $I(0) = 50$), with other initial conditions being given by $S(0) = 44.6 \times 10^6$ and $R(0) = 0$.

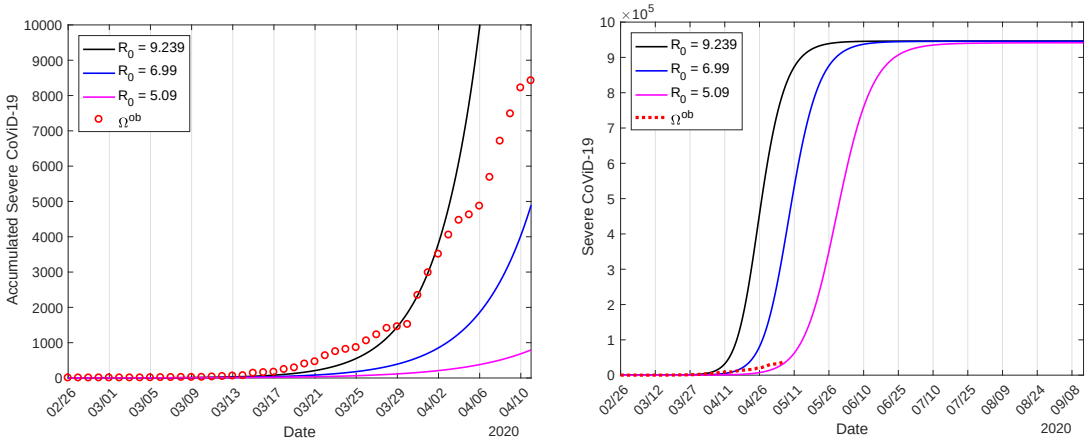

(a) (b)

Figure 3: The estimated curve of D_2 and observed data, plus two curves with lower transmission rates: $\beta_y = 0.59$ and $\beta_o = 0.679$ $(days^{-1})$, with $R_0 = 6.99$, and $\beta_y = 0.43$ and $\beta_o = 0.495$ $(days^{-1})$, with $R_0 = 5.09$ (a); and extended curves of accumulated number of severe CoViD-19 Ω (b).

Let us estimate the critical size of population (all persons are susceptible) N^{th} from equation (27). For $R_0 = 9.239$, we have $N^{th} = 4.83 \times 10^6$. Hence, for São Paulo State, isolating 39.77 million (89.2%) or above persons is necessary to avoid the persistence of epidemics. The number of young persons is 1.97 million less than the threshold number of isolated persons to guarantee eradication of CoViD-19.

3.1.2 Fitting the additional (fatality) mortality rates

We estimate taking into account confirmed deaths from February 26 (t_1) to March 31 (t_{35}), totalizing $n = 35$ observations, remembering that the first death occurred on March 16.

To estimate the mortality rates α_y and α_o, we fix the previously estimated transmission rates $\beta_y = 0.78$ and $\beta_o = 0.897$ (both in $days^{-1}$) for $R_0 = 9.239$, and evaluate the system of equations (2), (3) and (4), with initial conditions given by equation (7), to calculate, by varying α_y and α_o,

$$\sum_{i=1}^{n} \left[\Pi\left(t_i + \Delta\right) - \Pi^{ob}\left(t_i\right)\right]^2,$$

where Π is given by equation (14), with $\Pi(0) = 0$, and the time of death registration t_i portraits the deaths of new cases Δ times ago, that is, $D_2(t_i + \Delta)$. We minimize the sum of differences to estimate the fatality rates α_y and α_o letting $\alpha_y = 0.1\alpha_o$, due to the fact that the lethality among young persons is lower than elder persons [6], and by varying Δ and only α_o. The estimated delay is $\Delta = 9$ $days$, and fatality rates are $\alpha_y = 0.00053$ and $\alpha_o = 0.0053$ (both in $days^{-1}$).

Figure 4 shows the estimated curve of Π (a), and the extended curves of the number of CoViD-19 deaths (Π_y, Π_o, and $\Pi = \Pi_y + \Pi_o$) from equation (14) (b). The estimated curves Π_y,

Π_o, and $\Pi = \Pi_y + \Pi_o$ reach plateaus, and on September 13 the values are $3,820$ (0.63%), $34,110$ (10%) and $37,930$ (3.98%), respectively for, young, elder and total persons. The percentage between parentheses is the ratio Π/Ω, Ω being given in Figure 3(b).

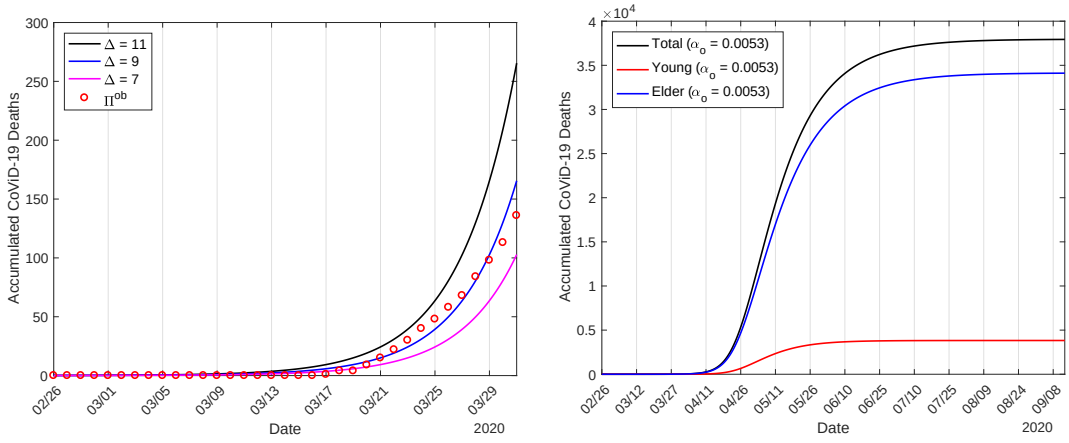

(a) (b)

Figure 4: The estimated curve of Π and the observed data for $R_0 = 9.239$ (a), and the accumulated number of CoViD-19 deaths (Π_y, Π_o, and $\Pi = \Pi_y + \Pi_o$) (b).

3.1.3 Estimating the proportion of isolated persons

We fix the transmission rates $\beta_y = 0.78$ and $\beta_o = 0.897$ (both in $days^{-1}$), giving $R_0 = 9.239$, and lower estimates for the mortality rates, $\alpha_y = 0.00053$ and $\alpha_o = 0.0053$ (both in $days^{-1}$), to estimate isolation (described by proportions k_y and k_o) of susceptible persons as control mechanism. Isolation was introduced on March 24, and we will estimate taking into account the confirmed cases until April 21, totalizing 29 observations. In this section, we do not consider future release, but only isolation initiated on March 24. The mean proportion of persons in isolation from March 24 to May 3 is $k_{mean} = 0.528$ (see Figure 2)

Here, we estimate the control variables by varying k_y and k_o. The system of equations (2), (3), and (4) is evaluated, with initial conditions (on February 26) given by equation (7) and boundary conditions (on March 24) given by equations (8) and (9), and we calculate the sum of square differences

$$\sum_{i=1}^{n} \left[\Omega\left(t_i\right) - \Omega^{ob}\left(t_i\right)\right]^2,$$

where t_1 is March 24 and t_{29} is April 21. We assume $k = k_y = k_o$ and varied $k = 0$, 0.4, 0.528, 0.6, 0.7, and 0.8, from which we observe that $k = 0.4$ and 0.6 fit parts of observed data, while $k = 0.7$ does not. Hence, we chose $k = k_{mean} = 0.528$ as the better estimated value. Figure 5(a) shows the curves of Ω with different proportions in isolation in São Paulo State and CoViD-19 observed data, and 5(b), the extended curves.

As we have pointed out above in the description of data (see Figure 2), the proportion in isolation delayed in approximately 9 days indeed affected the daily incidence of CoViD-19.

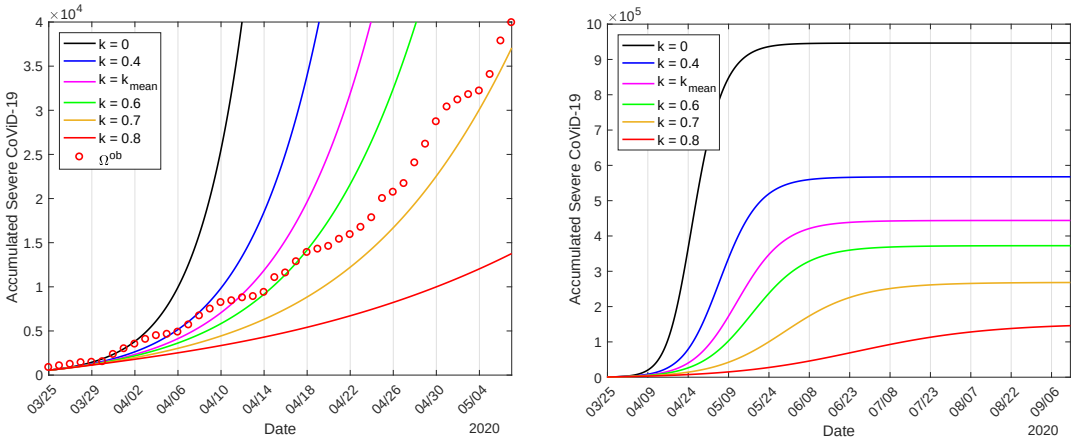

(a) (b)

Figure 5: The proportions in isolation in São Paulo State with CoViD-19 observed data (a), and the extended curves (b).

Also, the estimated proportion agrees with the mean value of proportions in isolation in São Paulo State. To be faithful with the trend indicated by data, we estimated taking into account data from March 24 to April 21. From Figure 5(b), Ω approaches plateau, and the asymptotic values on September 13 for $k = 0$, 0.4, 0.528, 0.6, 0.7, and 0.8 are, respectively, 9.646×10^5, 5.676×10^5 (59.97%), 4.44×10^5 (46.91%), 3.725×10^5 (39.36%), 2.682×10^5 (28.34%) and 1.46×10^5 (15.43%). The percentage between parentheses is the ratio $\Omega(k)/\Omega(0)$.

Figure 6 shows the estimated curves of Ω_y, Ω_o, and $\Omega = \Omega_y + \Omega_o$ (a) and Π_y, Π_o, and $\Pi = \Pi_y + \Pi_o$ (b), for $k = 0.528$. On September 13, the curves of accumulated cases and deaths of CoViD-19 approach asymptote. For $k = 0.528$, the curves Ω_y, Ω_o, and Ω attain asymptote values, respectively, 2.836×10^5 (46.85%), 1.603×10^5 (47%) and 4.44×10^5 (46.91%); and Π_y, Π_o and Π attain, respectively, $1,791$ (0.63%), $16,010$ (9.99%) and $17,800$ (4%). The percentages between parentheses are the ratios $\Omega\left(k_{mean}\right)/\Omega(0)$ and Π/Ω.

3.1.4 Estimating in the reduction of transmission rates

On April 13, 20 days after the beginning of isolation, we observe the first point completely untouching the curve (on April 12 leaving from curve begins). This new trend can not be explained by increased proportion in isolation (see Figure 5). To take into account this new tendency of data, in [31] we hypothesize that the using of face mask, constant hygiene (washing hands with alcohol and gel, and protection of mouth, nose and eyes, etc.) and other protection actions may decrease the infection. Based on evidence in literature [9], we assume that these actions reduce the force of infection by decreasing the transmission rates.

We fix the transmission rates $\beta_y = 0.78$ and $\beta_o = 0.897$ (both in $days^{-1}$), giving $R_0 = 9.239$, lower estimates for the mortality rates, $\alpha_y = 0.00053$ and $\alpha_o = 0.0053$ (both in $days^{-1}$), and proportion in isolation of susceptible persons $k = 0.528$, to estimate the protection factor ε.

Let us assume that on April 4 (9 days before initiating the effects), 11 days after the beginning of isolation, protection actions were adopted by persons, which reduce transmission

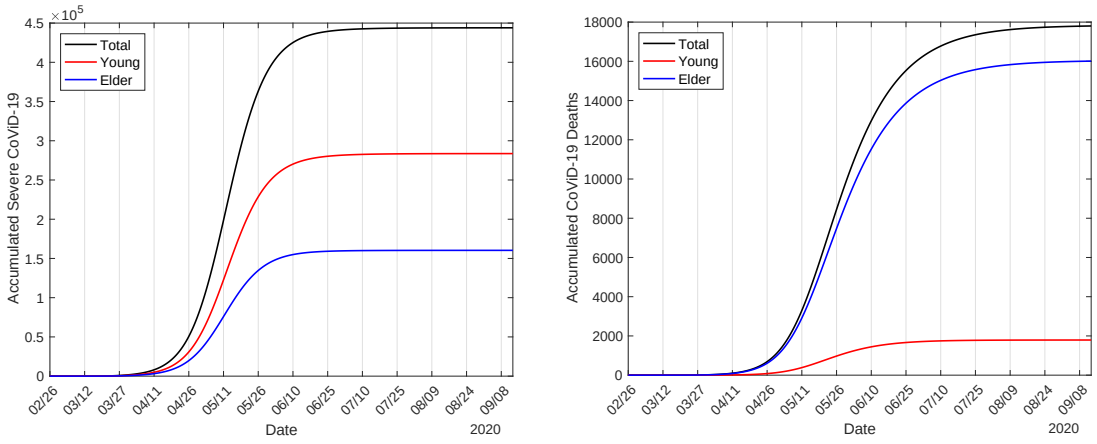

(a) (b)

Figure 6: The estimated curves of Ω_y, Ω_o, and $\Omega = \Omega_y + \Omega_o$ (a), and Π_y, Π_o, and $\Pi = \Pi_y + \Pi_o$ (b), for $k = 0.528$.

rates from β_y and β_o to $\beta'_y = \varepsilon_y \beta_y$ and $\beta_o = \varepsilon_o \beta'_o$, see equation (1). The system of equations (2), (3), and (4) is evaluated, with initial conditions (February 26) given by equation (7), and boundary conditions (March 24) given by equations (8) and (9), and we calculate the sum of square differences

$$\sum_{i=1}^{n} \left[\Omega\left(t_i\right) - \Omega^{ob}\right]^2,$$

by varying $\varepsilon = \varepsilon_y = \varepsilon_o$ in the interval between April 4 (t_1) and May 7 (t_{34}), totalizing 34 observations. We considered $\varepsilon = 0.8$, 0.7, 0.6, 0.5 and 0.4, and the better estimated value is $\varepsilon = 0.5$, hence $\beta'_y = 0.5\beta_y$. Figure 7(a) shows curves of Ω and observed data, where $\beta'_y = 0.8\beta_y = 0.624$, $0.7\beta_y = 0.546$, $0.6\beta_y = 0.468$, $0.5\beta_y = 0.39$ and $0.4\beta_y = 0.312$ (all in $days^{-1}$), plus $\varepsilon = 1$ and without isolation ($k = 0$). Figure 7(b) shows extended curves of Ω for 4 different decreasing values of transmission rates plus $\varepsilon = 1$.

The better fitting was $\varepsilon = 0.5$ from Figure 7(a). Notice that we did not use the same argument used to chose proportion in isolation k, because $\varepsilon = 0.4$ between two curves passing through observed points is worse than $\varepsilon = 0.5$. From Figure 7(b), Ω approaches plateau, and the asymptotic values on November 2 for $\varepsilon = 1$, 0.7, 0.6, 0.5 and 0.4 are, respectively, 4.44×10^5, 4.279×10^5 (96.37%), 4.135×10^5 (93.13%), 3.867×10^5 (87.09%) and 3.312×10^5 (74.59%). The percentage between parentheses is the ratio $\Omega(\varepsilon)/\Omega(0)$.

Figure 8 shows the estimated curves of Ω_y, Ω_o, and $\Omega = \Omega_y + \Omega_o$ (a) and Π_y, Π_o, and $\Pi = \Pi_y + \Pi_o$ (b), for $k = 0.528$ and $\varepsilon = 0.5$, that is, $\beta'_y = 0.39$ and $\beta'_o = 0.4485$, reducing the basic reproduction number to $R_0 = 4.62$. On November 2, the curves of accumulated cases and deaths of CoViD-19 approach plateaus. In this case, the curves Ω_y, Ω_o, and Ω attain asymptotic values, respectively, 2.438×10^5 (85.97%), 1.428×10^5 (89.08%) and 3.867×10^5 (87.09%); and Π_y, Π_o and Π attain, respectively, $1,540$ (0.632%), $14,240$ (9.97%) and $15,780$ (4.08%). The percentages between parentheses are the ratios $\Omega\left(\varepsilon = 0.5\right)/\Omega(\varepsilon = 1)$ and Π/Ω.

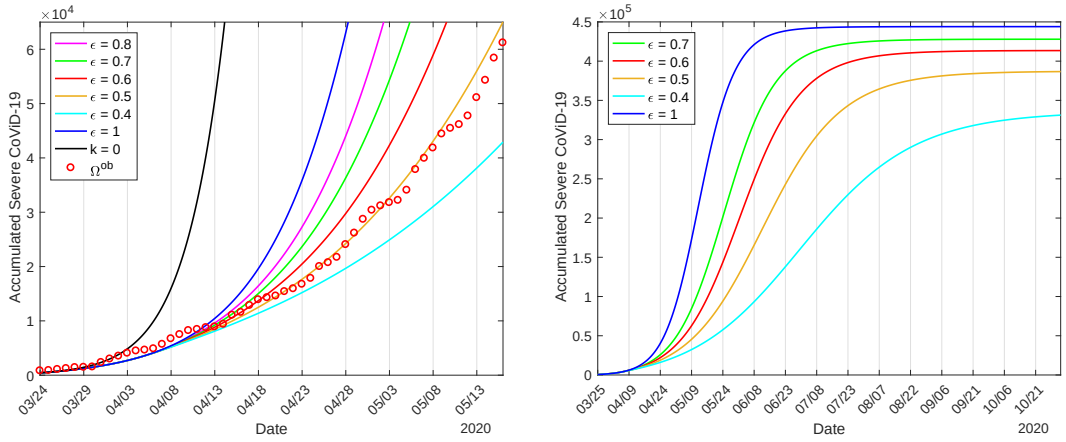

(a) (b)

Figure 7: The curves of $D_2 = D_{2y} + D_{2o}$ and observed data, where $\beta'_y = 0.8\beta_y = 0.648$, $0.7\beta_y = 0.567$, $0.6\beta_y = 0.486$, $0.5\beta_y = 0.405$ and $0.4\beta_y = 0.324$, plus $\beta'_y = 1$ and without isolation (a), and extended curves of D_2 for 4 different decreasing values of transmission rates plus $\beta'_y = 1$ (b).

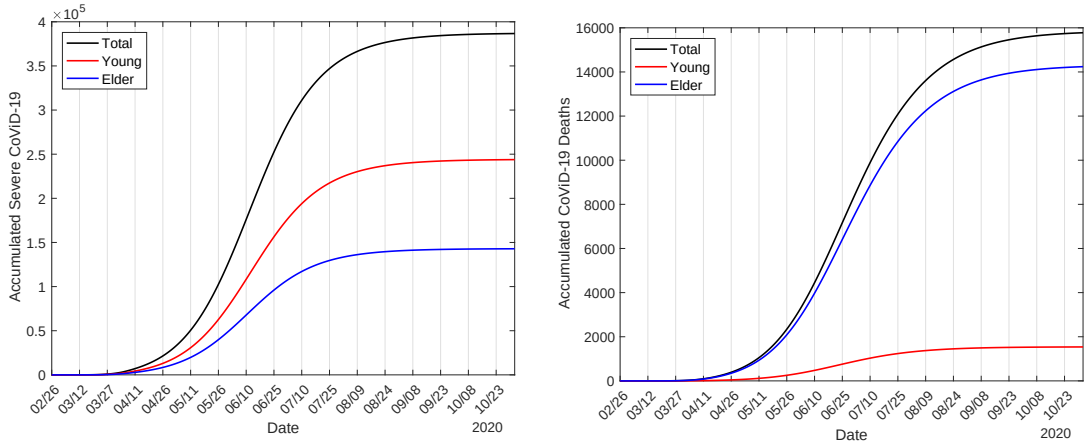

(a) (b)

Figure 8: The estimated curves of Ω_y, Ω_o, and $\Omega = \Omega_y + \Omega_o$ (a) and Π_y, Π_o, and $\Pi = \Pi_y + \Pi_o$ (b), for $k = 0.528$ and $\varepsilon = 0.6$. The reduced transmission rates are $\beta'_y = 0.486$ and $\beta'_o = 0.559$, with $R_0 = 5.76$.

3.2 Current epidemiological scenario

Before presenting epidemiological scenarios considering releasing strategies, we present the current epidemiological scenario using all previously estimated parameters: The transmission rates $\beta_y = 0.78$ and $\beta_o = 0.897$ (both in $days^{-1}$), giving $R_0 = 9.239$; the fatality rates $\alpha_y = 0.00053$ and $\alpha_o = 0.0053$ (both in $days^{-1}$); the proportion in isolation of susceptible persons $k = 0.528$; and the protection factor $\varepsilon = 0.5$ reducing the transmission rates to $\beta'_y = 0.39$ and $\beta'_o = 0.4485$

(both in $days^{-1}$), giving $R_0 = 4.62$. Hereafter, all these values are fixed, unless explicitly cited.

In Figure 9 we show the effects of interventions on the dynamics of new coronavirus. As interventions are added (isolation followed by protection actions), we observe decreasing in the peaks of hospitalized CoViD-19 D_2, which move to the right Figure 9(a) shows the curves representing $k = 0$ and $\varepsilon = 1$ (without interventions), $k = 0.528$ and $\varepsilon = 1$ (only isolation), and $k = 0.528$ and $\varepsilon = 0.5$ (isolation and protection). In Figure 9(b) we show the number of immune persons I corresponding to three cases shown in Figure 9(a). The curves follow sigmoid-shape.

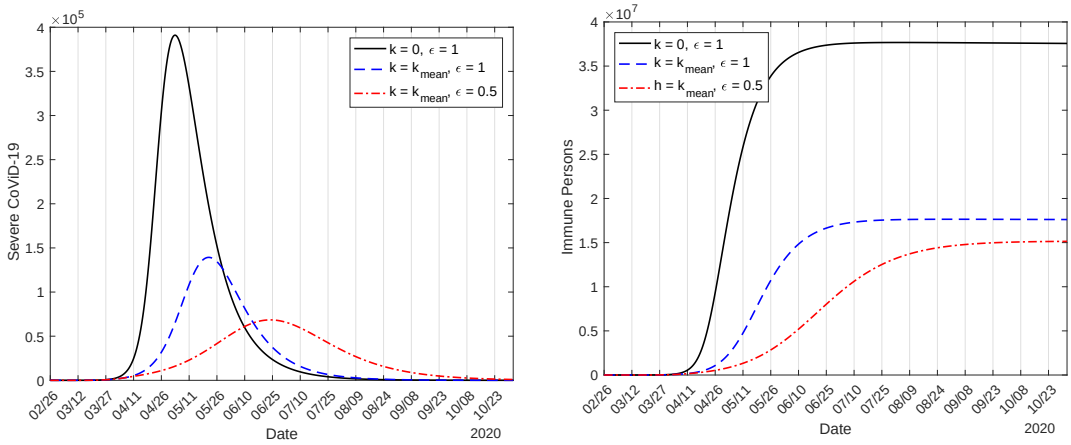

Figure 9: The effects of intervention on the dynamics of new coronavirus from without interventions ($k = 0$ and $\varepsilon = 1$), only isolation ($k = 0.528$ and $\varepsilon = 1$), and isolation plus protection ($k = 0.528$ and $\varepsilon = 0.6$) (a), and number of immune persons corresponding to three cases.

When there are not any interventions ($k = 0$ and $\varepsilon = 1$), the numbers of immune persons I_y, I_o, and I increase from zero to, respectively, 3.53×10^7, 6.108×10^6 and 4.143×10^7 on June 1 (figure not shown). When interventions are adopted, the numbers are, on June 1, 3.687×10^6 (10.44%), 0.6903×10^6 (11.3%) and 4.377×10^6 (10.56%). Figure 9(b) showed only I with and without interventions. The percentage between parentheses is the ratio between with and without interventions $I(k, \varepsilon)/I(0, 1)$ on June 1. The isolation will end on May 31, and on June 1 will begin release.

Let us compare the peaks of D_2. When there are not any interventions ($k = 0$ and $\varepsilon = 1$), the peaks for young, elder and total persons are, respectively, 2.266×10^5, 1.648×10^5, and 3.91×10^5, occurring on May 2, 4 and 3. Considering isolation alone ($k = 0, 528$ and $\varepsilon = 1$), the peaks for young, elder and total persons are, respectively, $78,190$ (34.51%), $61,230$ (37.15%), and 1.393×10^5 (35.63%), which occur on May 21, 23, and 22. Considering interventions ($k = 0, 528$ and $\varepsilon = 0.5$), the peaks for young, elder and total persons are, respectively, $36,510$ (16.11%), $32,000$ (19.42%), and $68,460$ (17.5%), which occur on June 23, 25, and 23. The percentage between parentheses is the ratio between with and without interventions $D_2(k, \varepsilon)/D_2(0, 1)$.

The isolation does not change the basic reproduction number, and just after the end of isolation, the dynamics is driven by the original epidemics, reaching the non-trivial equilibrium

point P^* given by R_0. However, the reduction in the transmission rates decreases the basic reproduction number. Hence, from February 26 to April 3, the dynamics system is driven by $\beta_y = 0.78$ and $\beta_o = 0.897$ (both in $days^{-1}$, $R_0 = 9.239$), and since April 4, the dynamics is driven by $\beta'_y = 0.39$ and $\beta'_o = 0.4485$ (both in $days^{-1}$, $R_0 = 4.62$). If protection actions are abandoned, the dynamics is driven by the trend of $R_0 = 9.239$ again.

Due to isolation and protection, there are so many persons remained as susceptible. In Figure 10 we show circulating susceptible persons S_y, S_o and $S = S_y + S_o$ (a), and circulating plus isolated (to be infected when released) susceptible persons S_y^{tot}, S_o^{tot} and $S^{tot} = S_y^{tot} + S_o^{tot}$ (b), using equation (12). Remember that S_y^{tot} differs from S_y just after the introduction of isolation (March 24).

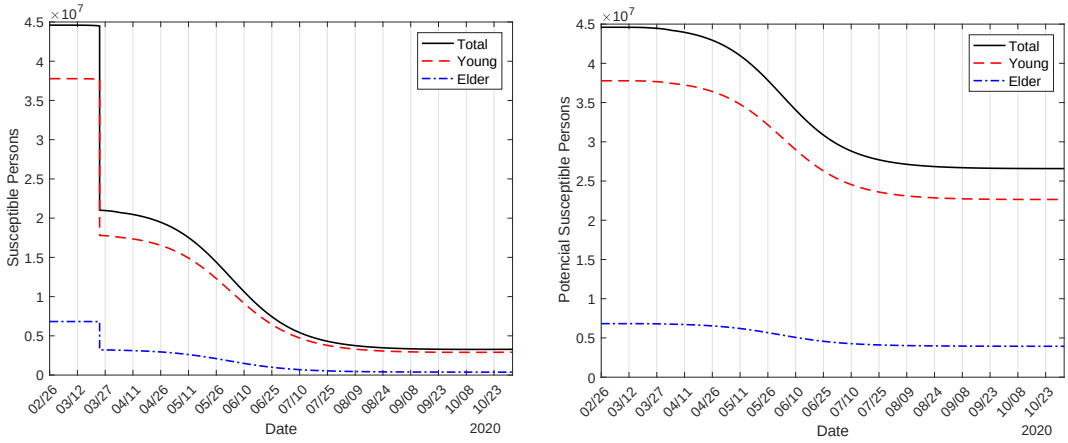

(a) (b)

Figure 10: The circulating susceptible persons S_y, S_o and $S = S_y + S_o$ (a), and potential susceptible persons to be infected S_y^{tot}, S_o^{tot} and $S^{tot} = S_y^{tot} + S_o^{tot}$ (b).

Let us compare the number of susceptible persons before and after the introduction of interventions, which will end on May 31. On June 1, when there are not any interventions ($k = 0$ and $\varepsilon = 1$), the numbers of susceptible persons S_y, S_o and $S = S_y + S_o$ are, respectively, $25,260$, 313 and $25,580$. When there are interventions, on June 1, the numbers of susceptible persons are 1.104×10^7 $(43,705\%)$, 1.847×10^6 $(590,095\%)$ and 1.289×10^7 $(50,391\%)$, for young, elder and total persons, respectively. For S_y^{tot}, S_o^{tot} and $S^{tot} = S_y^{tot} + S_o^{tot}$, we have, respectively, 3.09×10^7 $(122,328\%)$, 5.433×10^6 $(1,735,783\%)$ and 3.633×10^7 $(142,025\%)$. The percentage between parentheses is the ratio between with and without interventions $S(k,\varepsilon)/S(0,1)$ on June 1. With interventions, at the end of isolation, there are more than 437-times the number of susceptible young and total persons, and for elder persons, $5,900$-times, with respect to without interventions. However, if we add those under isolation to be released at this time, there are more than $1,220$-times the number of susceptible young and total persons, and for elder persons, $17,357$-times. Hence, the second wave without interventions will be intense, but infecting much more elder persons. In the absence of vaccine and effective treatment, interventions aiming reduction in the transmission must be continued for long time (maybe years to avoid intense second wave).

It is important to estimate the basic reproduction number, which portraits the beginning and ending phases of an epidemics [29]. During the evolving of epidemics, however, the effective reproduction number acts on the course of epidemics. We use the approximate effective reproduction number R_{ef}, given by equation (24), to follow the trend of dynamics, remembering that $R_{ef} > 1$ implies epidemics in expansion, while $R_{ef} < 1$, the contraction. Figure 11 illustrates the effective reproduction number R_{ef} with (a) and without (b) interventions, using equation (24), and the effects on the evolving of epidemics represented by D_2. To be fit together in the same frame with R_{ef}, the curve of D_2 is divided by $7,000$ (a) or $40,000$ (b). The curve of R_{ef} follows the shape of susceptible persons as shown in Figure 10, as expected.

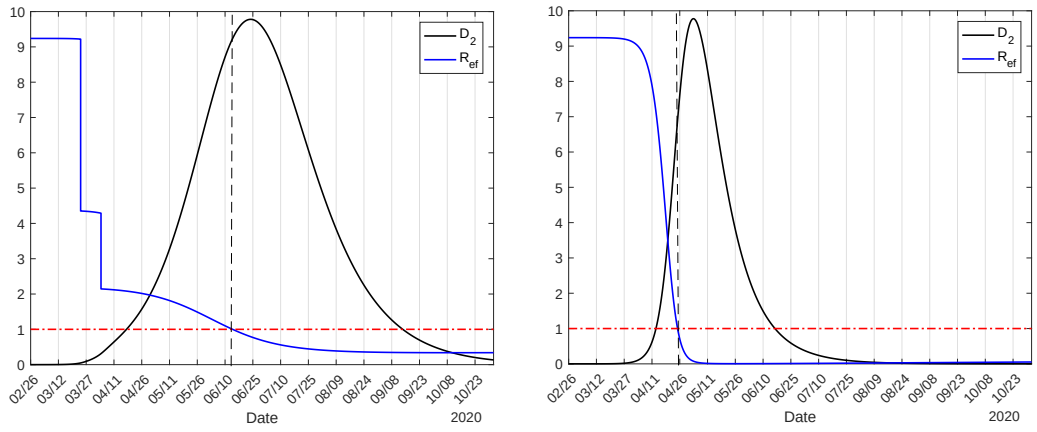

(a) (b)

Figure 11: Illustration of the effective reproduction number R_{ef} when isolation and protection are adopted (a) and without adoption (b), with the actual value of curve D_2 must be multiplied by, respectively, $7,000$ (a) and $40,000$ (b).

When epidemics evolves following its natural way (without interventions), on June 1 the effective reproduction number is very low ($R_{ef} = 0.0053$) in ascending phase of epidemics, while with interventions, $R_{ef} = 1.334$ also in ascending phase. As expected, $R_{ef} = 1$ occurs before the peak of epidemics, for this reason the value of R_{ef} lower than 1 also occurs in the ascending phase. This behavior, when there are not interventions, is due to huge number of infectious individuals, which is responsible to infect many susceptible persons, such as inertia maintains object in movement even though there are opposing forces. However, when interventions are acting on a community, Figure 11(a) shows $R_{ef} = 1$ occurring just before the peak of epidemics, in the ascending phase. Hence, further interventions, especially release, must take this behavior into account and do not assume that all descending phase is relatively safe. When R_{ef} is lower but near than 1, there is great possibility of rebounding of epidemics when release is initiated.

Let us estimate parameters related to the occupancy of beds in hospitals and counting the number of deaths.

We assumed that all CoViD-19 cases (D_2) need hospital care, hence we use $h_y = 1.0$ and $h_o = 1.0$. In Wuhan, China [16], 80.9% of infections did not need hospital care, 13.8% were severe (developing severe diseases including pneumonia and shortness of breath) and 4.7% were

critical (respiratory failure, septic shock, and multi-organ failure). From 4.7%, we use $h_1 = 0.05$, which is the proportion of hospitalized persons needing ICU care. However, we use higher values for elder and young persons, $h_{1o} = 0.25$ and $h_{1y} = 0.15$. For the ratio ICU:ICU/intubated, we use approximately 13.8% and 4.7%, resulting in $3:1$, and $h_2 = 1/4 = 0.25$, which is the proportion of ICU persons needing ICU/intubated care. However, we use higher and lower values for elder and young persons, $h_{2o} = 0.3$ and $h_{2y} = 0.2$. Finally, we assume that proportions not surviving in ICU/intubated are $h_{3y} = 0.5$ and $h_{3o} = 0.8$. Other parameters are given in Table 3, especially the proportion of deaths, which are estimated using equations (20), (21) and (22) and minimizing the sum

$$\sum_{i=1}^{n} \left[\Pi_s\left(t_i + \Delta\right) - \Pi^{ob}\left(t_i\right)\right]^2,$$

where $\Pi_s = \Pi_1 + \Pi_2 + \Pi_3$ is the sum of all deaths in hospital. The better estimation was obtained with $\Delta = 15$ days.

Let us estimate the occupancy of beds in hospitals, using equations (16), (17) and (18), the number of deaths, using equations (20), (21) and (22), and number of cured persons using equation (19).

We calculate the number of occupied beds due to CoViD-19. Figure 12 shows the number of beds occupied by young ($j = y$) (a) and elder ($j = o$) (b) for inpatients (B_{1j}), ICU (B_{2j}) and ICU/intubated (B_{3j}) persons.

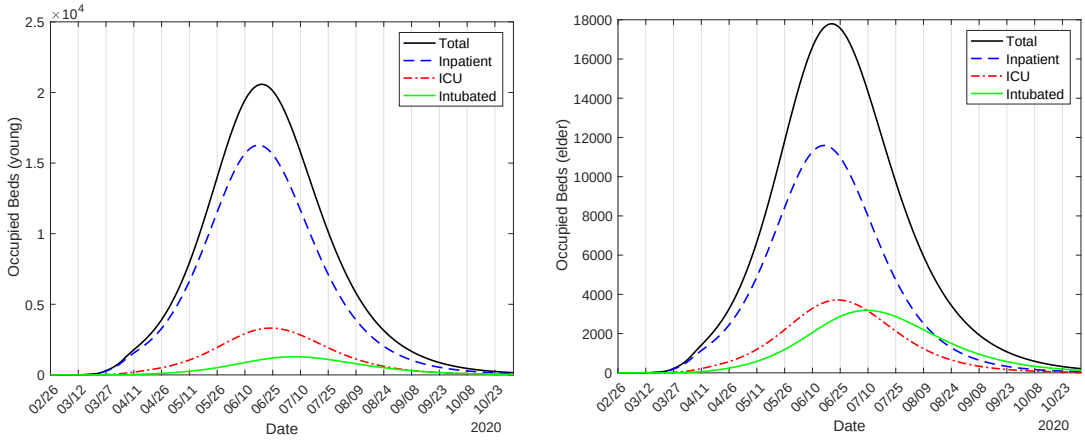

(a) (b)

Figure 12: The number of beds occupied by young ($j = y$) (a) and elder ($j = o$) (b) persons in hospital (B_{1j}), ICU (B_{2j}) and ICU/intubated (B_{3j}).

The peak of numbers of occupied beds for young inpatient, ICU, ICU/intubated and total persons are, respectively, $16,260$, $3,312$, $1,282$ and $20,580$, which occur on June 18, June 23, July 7 and June 19. For elder persons, we have, respectively, $11,590$, $3,714$, $3,184$ and $17,790$, which occur on June 16, June 24, July 9 and June 20.

We calculate the number of deaths due to CoViD-19. Figure 13 shows the number of deaths due to CoViD-19 by young ($j = y$) (a) and elder ($j = o$) (b) for inpatient (Π_{1j}), ICU (Π_{2j})

and ICU/intubated (Π_{3j}) persons. At the end of the first wave of epidemics, the numbers of deaths for young persons occurred in hospital, ICU, ICU/intubated and total are, respectively, $2,482$, $1,835$, 1.094 and $5,412$. For elder persons, we have, respectively, $7,169$, $5,358$, $4,953$ and $17,480$. In General Hospital of the Medical School of the University of São Paulo, on May 14, died persons are 17% of all CiViD-19 patients.

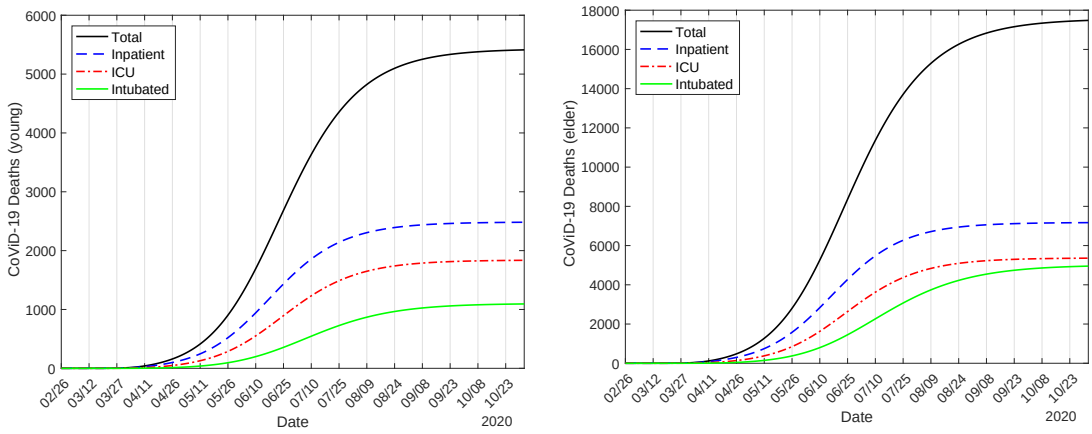

Figure 13: The number of deaths due to CoViD-19 by young ($j = y$) (a) and elder ($j = o$) (b) persons in hospital (Π_{1j}), ICU (Π_{2j}) and ICU/intubated (Π_{3j}).

We used $\Delta = 9$ days to estimate the fatality rates. However, if we use $\Delta = 15$ days, the estimated fatality rates are $\alpha_y = 0.0009$ and $\alpha_o = 0.00009$ (both in $days^{-1}$), resulting at the end of the first wave of epidemics the numbers of deaths for young, elder and total persons, respectively, 263, $2,641$ and $2,904$. Hence, the delayed time Δ for estimating fatality rates is different to the fatality expressed in proportions.

We calculate the number of cured persons $C = C_y + C_o$. Figure 14 shows the number of cured from CoViD-19 by young C_y, elder C_o, and all persons (a) in the beginning of epidemics, and extended curves (b). At the end of the first wave of epidemics, the numbers of cured from CoViD-19 by young C_y, elder C_o, and all persons are, respectively, 2.371×10^5, 1.245×10^5, and 3.616×10^5.

The number of cured persons is 93.5% of all severe CoViD-19 cases $\Omega = 3.867 \times 10^5$ (Figure 7(b)), and 1579.6% of deaths at the end of the first wave of epidemics. In General Hospital of the Medical School of the University of São Paulo, on May 14, the cured persons are 51.5% of all CiViD-19 patients, and 340% of deaths.

On June 1, the São Paulo State authorities will release isolated persons. Based on estimated parameters, we calculate the number of occupied beds and deaths due to CoVid-19 considering three scenarios: without any interventions ($k = 0$ and $\varepsilon = 1$), isolation alone ($k = 0.528$ and $\varepsilon = 1$), and isolation plus protection ($k = 0.528$ and $\varepsilon = 0.5$). In Table 4 we summarize the decreasing in the number of occupied beds and deaths due to CoVid-19 on June 1. The percentage between parentheses is the ratio between with and without interventions $B(k, \varepsilon)/B(0, 1)$ and $\Pi(k, \varepsilon)/\Pi(0, 1)$.

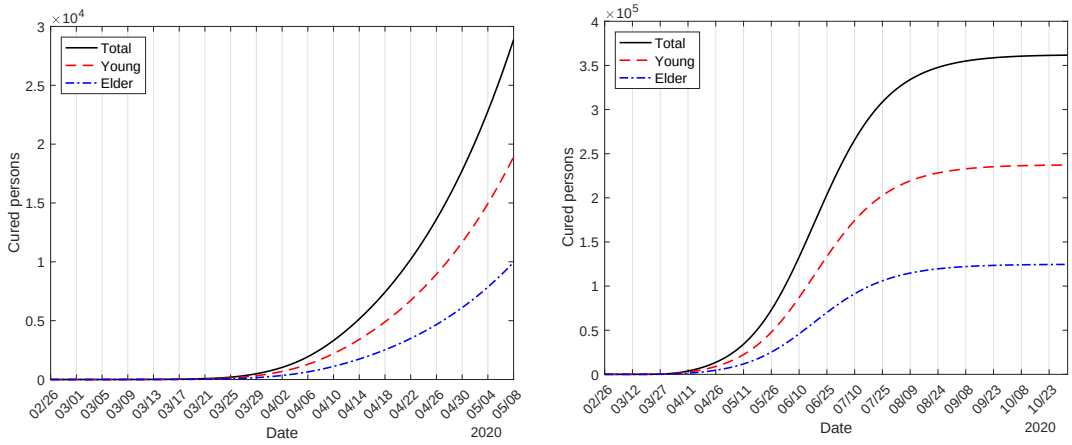

(a) (b)

Figure 14: The numbers of cured young, elder and total persons from CoViD-19 (a), and extended curves (b).

Table 4: The summary of the decreasing in the number of occupied beds and deaths due to CoVid-19 on June 1, with $k_{mean} = 0.528$. The percentage between parentheses is the ratio between with and without interventions $B(k,\varepsilon)/B(0,1)$ and $\Pi(k,\varepsilon)/\Pi(0,1)$.

	B_{1y}	B_{2y}	B_{3y}	B_y	Π_{1y}	Π_{2y}	Π_{3y}	Π_y
$k=0$ $\varepsilon=1$	123,700	21600	6418	145500	6154	4518	2397	13069
$k=k_m$ $\varepsilon=1$	38570 (31.2%)	7331 (33.9%)	2440 (33%)	46970 (32.3%)	2744 (44.6%)	1894 (42%)	831 (28%)	5469 (42.1%)
$k=k_m$ $\varepsilon=0.5$	13490 (10.9%)	2356 (10.9%)	650 (10.1%)	16500 (11.3%)	1139 (18.5%)	683 (15%)	256 (10.7%)	2078 (15.9%)
	B_{1o}	B_{2o}	B_{3o}	B_o	Π_{1o}	Π_{2o}	Π_{3o}	Π_o
$k=0$ $\varepsilon=1$	81640	21960	13760	106700	17100	12620	9494	39214
$k=k_m$ $\varepsilon=1$	26330 (32.3%)	7768 (35.4%)	5401 (39.3%)	36890 (34.6%)	7696 (45%)	5300 (42%)	3201 (33.7%)	16197 (41.3%)
$k=k_m$ $\varepsilon=0.5$	9810 (12%)	2661 (12.1%)	1515 (11%)	13990 (13.1%)	3413 (20%)	2016 (16%)	1034 (10.9%)	6463 (16.5%)

Observe that isolation alone decreased occupancy of beds and deaths to 30-45%, while the addition of protection actions decreased to 10-20%.

3.2.1 Daily CoViD-19 from estimated accumulated cases

We used accumulated data shown in Figure 2(b) and Ω given by equation (13) to estimate the transmission rates β_y and β_o, the proportion in isolation k, and protection actions ε. The curve labelled $\varepsilon = 0.5$ in Figure 7(b) is the estimated curve Ω, from which the severe cases D_2 was

derived, corresponding to the most flattened curve shown in Figure 9(a). From that curve we derive the daily cases Ω_d calculated by equation (15). In Figure 15(a) we show the calculated curve Ω_d and daily cases presented in Figure 2(b). In Figure 15(b) we show initial part of estimated Ω with observed data Ω^{ob}, the extended Ω_d and daily observed cases Ω_d^{ob}, and severe cases D_2. The peaks of D_2 and Ω_d occur, respectively, on June 23 and 12.

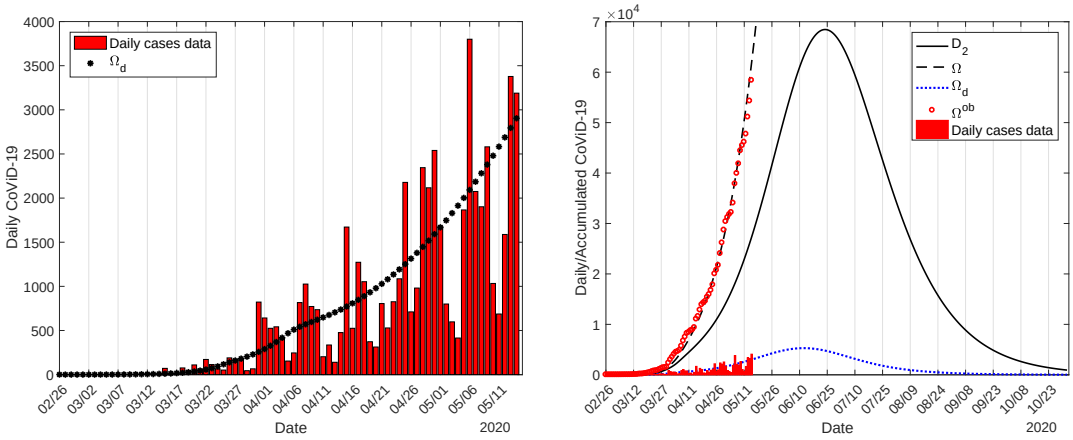

(a) (b)

Figure 15: The fitted curve of ΔD_2 with accumulated cases data (a), and the extended curve ΔD_2 with previously adjusted D_2 (b).

On June 12, the peak of the daily cases of CoViD-19 predicted by estimated values of parameters reaches $5,287$, remembering that the peak of D_2 on June 23 is $68,460$. However, on June 23, the number of accumulated cases is 2.43×10^5, which is 63% of cases at the final of the first wave of epidemics 3.867×10^5.

3.2.2 Subnotification along epidemics

Let us discriminate the circulation of the new coronavirus in a community according to infected classes. Figure 16 shows all persons harboring this virus (E_j, A_j, D_{1j}, Q_{2j} and D_{2j}), for young ($j = y$) (a) and elder ($j = o$) (b) persons. Notice that $Q_{1j} = Q_{3j} = 0$ (there is not mass testing available during the first wave of epidemics).

Let us assess the subnotification of CoViD-19, considering the ratio hidden:apparent. We classify all who harbor the new coronavirus (exposed, asymptomatic and not manifesting) in the hidden category, and in the apparent category, all who manifest symptoms. Hence, the ratio is calculated as $(E_j + A_j + D_{1j})/(Q_{2j} + D_{2j})$. In Figure 17(a) we show the ratio hidden:apparent based on Figure 17 for young ($j = y$), elder ($j = o$) and total persons. On February 26 ($t = 0$), the ratio was $10 : 1$ for young and elder persons due to initial conditions. Aiming comparison, Figure 17(b) shows the ratio hidden:apparent when there are not any intervention.

Figure 17(b) portraits the tendency of subnotifications in the sense of hidden:apparent when there are not interventions. There is a quick increasing following ascending phase of epidemics, reaching a plateau for a while, and then decreases quickly, reaching an asymptote. When

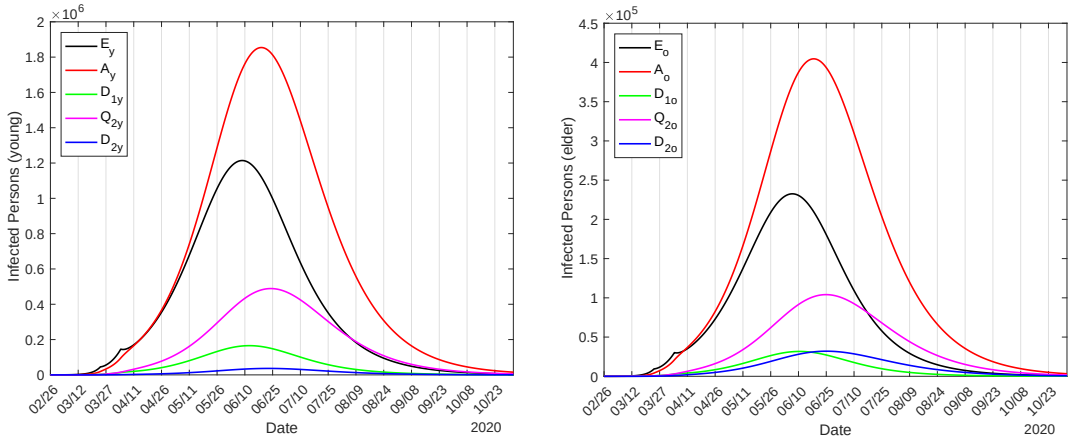

(a) (b)

Figure 16: All persons harboring the new coronavirus (E_j, A_j, D_{1j}, Q_{2j} and D_{2j}), for young ($j = y$) (a) and elder ($j = o$) (b) persons.

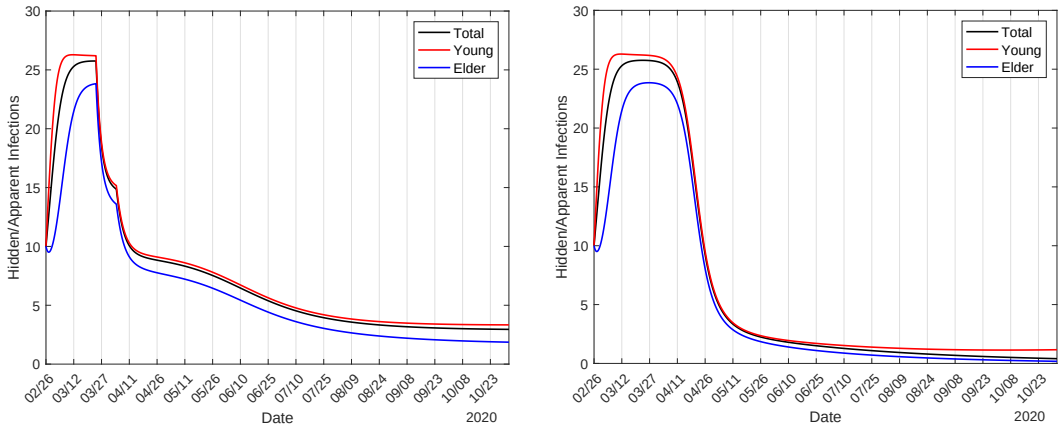

(a) (b)

Figure 17: The ratio hidden:apparent based on Figure 16, calculated based on the ratio $(E + A + D_1) : (Q_2 + D_2)$. The ratio hidden:apparent when there is not any intervention is shown (b).

interventions are introduced, subnotification changes behavior, following the sequential introduction of interventions: There is first perturbation, which occurs at the moment when isolation is introduced, followed by a second perturbation, when protection is introduced. Comparing Figures 16 and 17(a), as the epidemics evolves, the ratio increases quickly in the beginning, reaches a plateau during the increasing phase, and decreases during the declining phase, finally reaching another plateau after the ending phase of the first wave. In the first plateau, the ratios are 24 : 1, 27 : 1, and 26 : 1 for, respectively, elder, young, and total persons. At the end of the first wave, subnotification reaches asymptotically the ratio 1 : 1 when there are not interventions (2 : 1 with intervention). Therefore, during epidemics, there are much more

hidden than apparent persons, which makes any control mechanisms hard if mass testing could not be implemented. However, the estimation of the ratio between hidden and apparent cases can be helpful in designing mass testing aiming to isolate asymptomatic persons.

3.2.3 Epidemics among isolated persons

We evaluated spread of new coronavirus among isolated persons. We also evaluate the effects of lockdown implemented belatedly.

Isolation – transmission among isolated persons As we have pointed above, when isolation is done lately, among isolated persons there will be persons harboring virus. Just before the beginning of isolation on March 24, the numbers of persons in each class, for $k = 0.528$, are

$$\text{young} \begin{cases} S_y = 1.779 \times 10^7, & Q_y = 1.99 \times 10^7, & E_y = 4.542 \times 10^4, & A_y = 1.925 \times 10^4, \\ D_{1y} = 3.183 \times 10^3, & Q_{2y} = 2.395 \times 10^3, & D_{2y} = 2.31 \times 10^2 \end{cases}$$
$$\text{elder} \begin{cases} S_o = 3.213 \times 10^6, & Q_o = 3.594 \times 10^6, & E_o = 9.434 \times 10^3, & A_o = 4.153 \times 10^3, \\ D_{1o} = 6.01 \times 10^2, & Q_{2o} = 5.57 \times 10^2, & D_{2o} = 1.659 \times 10^2, \end{cases}$$

with $Q_{1y} = Q_{1o} = 0$ and $I = 1.0032 \times 10^4$.

To estimate the circulation of virus among isolated persons, we simulate the system of equations (2), (3), and (4) taking as initial conditions the number of persons in each class: $S_y = Q_y = 1.99 \times 10^7$, $S_o = Q_o = 3.594 \times 10^6$, $Q_y = Q_o = 0$, and for all other variables, we assume half of the corresponding values just before March 24. Figure 18 shows the curves of D_{2y}, D_{2o}, and $D_2 = D_{2y} + D_{2o}$ for $\beta'_y = \beta_y/5 = 0.156\ days^{-1}$, with $R_0 = 1.848$ (a), and $\beta''_y = \beta_y/10 = 0.078\ days^{-1}$, with $R_0 = 0.924$ (b), from March 24 to May 31, during the period of isolation. On June 1, the numbers of severe CoViD-19 cases are, $4,632$, $3,990$ and $8,622$, respectively, for young, elder, and total persons for $R_0 = 1.848$; and 316, 366 and 642, for $R_0 = 0.924$. For $k = 0.528$ and $R_0 = 0.924$, this 0.94% additional CoViD-19 cases compared to the peak of cases among circulating persons $(68,460)$ is negligible, however for $R_0 = 1.848$, the 12.6% additional CoViD-19 cases are not negligible on June 1. Nevertheless, when these isolated infectious individuals are released, they contribute to increase the velocity of propagation.

The virus should be circulating among isolated persons through restricted contact occurring in the household and/or neighborhood. If pre-symptomatic persons could be transferred quickly to hospital, it is expected that asymptomatic persons are predominantly spreading the new coronavirus. If we assume that they are releasing a low amount of virus, it is expected that more asymptomatic cases will arise than severe CoViD-19. There is a proportional decreasing in susceptible persons as immune persons increase, resulting in the decrease in the effective reproduction number, which is the herd immunity phenomenon.

Lockdown – Transmission among locked-down persons As in isolation, when lockdown is done belatedly, among isolated persons by lockdown there will be persons harboring virus. Among these locked-down persons, depending on the epidemiological status, there will be a higher number of persons harboring virus, as well as elder persons will be now in close contact with infectious young persons. As we have pointed out in [30] [31], the presence of infectious young persons increase hugely the risk of elder persons.

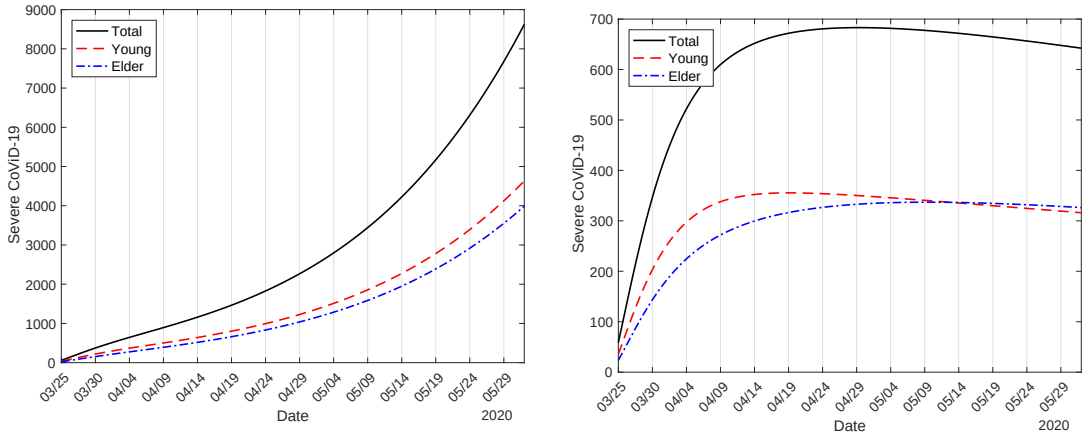

Figure 18: The curves of D_{2y}, D_{2o}, and $D_2 = D_{2y} + D_{2o}$ for $\beta'_y = \beta_y/5 = 0.162$, with $R_0 = 1.919$ (a), and $\beta''_y = \beta_y/10 = 0.081$, with $R_0 = 0.96$ (b), from March 24 to May 11, during the period of isolation.

We illustrate lockdown using epidemiological scenarios of São Paulo State under interventions (isolation $k = 0.528$ and reduction $\varepsilon = 0.5$), and supposing that on May 10 lockdown is implemented. In general, lockdown lasts for few days, for instance, we let 14 days, and high proportion in isolation, for instance, $k = 0.9$. On May 10, just before the beginning of lockdown, the numbers of circulating persons in each class are

$$\text{young} \begin{cases} S_y = 1.491 \times 10^7, & Q_y = 1.987 \times 10^7, & E_y = 6.78 \times 10^5, & A_y = 7.409 \times 10^5, \\ D_{1y} = 8.053 \times 10^4, & Q_{2y} = 1.617 \times 10^5, & D_{2y} = 1.251 \times 10^4 \end{cases}$$
$$\text{elder} \begin{cases} S_o = 2.614 \times 10^6, & Q_o = 3.588 \times 10^6, & E_o = 1.375 \times 10^5, & A_o = 1.665 \times 10^5, \\ D_{1o} = 1.639 \times 10^4, & Q_{2o} = 3.399 \times 10^4, & D_{2o} = 1.041 \times 10^4, \end{cases}$$

with $Q_{1y} = Q_{1o} = 0$ and $I = 1.577 \times 10^6$. However, the isolated susceptible persons on March 24 ($S_y = Q_y = 1.99 \times 10^7$, $S_o = Q_o = 3.594 \times 10^6$ and zero for all other classes) decreased by natural mortality μ, and on March 10, they are $S_y = 1.987 \times 10^7$ and $S_o = 3.588 \times 10^6$.

Our task is evaluating the transmission among locked-down persons, which are summed with the isolated susceptible persons on May 10, by simulating the system of equations (2), (3), and (4). The boundary conditions on May 10 (denoted by x) is given by equation (8) for all classes with $k = 0.9$, recalling that in isolated population we assumed that there are only susceptible persons. Hence, the boundary conditions supplied to the system of equation driving persons in isolation and lockdown are

$$\text{young} \begin{cases} S_y(x) = 3.329 \times 10^7, & Q_y(x) = 0, & E_y(x) = 6.102 \times 10^5, & A_y(x) = 6.668 \times 10^5, \\ D_{1y}(x) = 7.248 \times 10^4, & D_{2y}(x) = 0, & Q_{2y}(x) = 1.456 \times 10^5 \end{cases}$$
$$\text{elder} \begin{cases} S_o(x) = 5.941 \times 10^6, & Q_o(x) = 0, & E_o(x) = 1.238 \times 10^5, & A_o(x) = 1.499 \times 10^5, \\ D_{1o}(x) = 1.475 \times 10^4, & D_{2o}(x) = 0, & Q_{2o}(x) = 3.059 \times 10^4, \end{cases}$$

with $Q_{1y}(x) = Q_{1o}(x) = 0$ and $I(x) = 1.419 \times 10^6$. Remember that severe CoViD-19 are hospitalized, hence $D_{2y}(x) = D_{2o}(x) = 0$.

In Figure 19 we illustrate the introduction of 14 days lockdown. We assume that the protection factor is $\varepsilon = 0.5$ during isolation and lockdown, but the transmission rates are reduced to factor 5, that is, $\beta_y' = \beta_y/5 = 0.156$ and $\beta_o' = \beta_o/5 = 0.179$ (both in $days^{-1}$), with $R_0 = 0.9239$ (a), and $\beta_y' = \beta_y/3 = 0.26$ and $\beta_o' = \beta_o/3 = 0.299$ (both in $days^{-1}$), with $R_0 = 1.5398$ (b). We present the curves of D_{2y}, D_{2o}, and D_2 with isolation only (dashed) and with isolation and lockdown (continuous). The values of for young, elder, and total persons in isolation alone on May 10 are, respectively, $12,080$, $10,020$ and $22,120$, and on May 24, $21,880$, $18,350$ and $39,980$. Hence, the differences between May 24 and 10 are $9,800$, $8,330$ and $17,860$, respectively, for young, elder, and total persons. In isolation followed by lockdown, the number of severe CoViD-19 cases increased from 0 to values given in Table 5, on May 24.

Figure 19

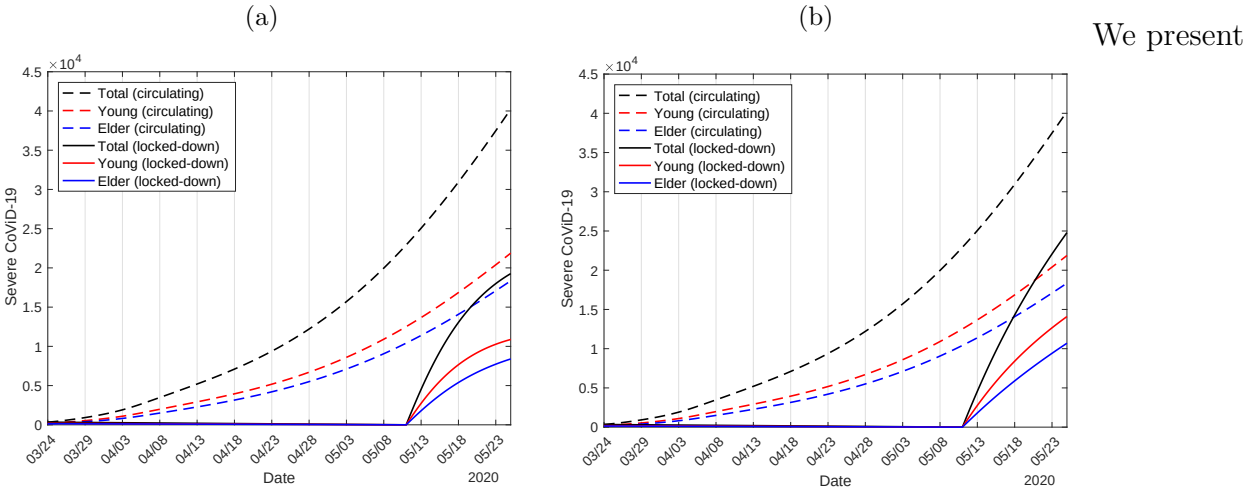

We present the curves of D_{2y}, D_{2o}, and D_2 considering the protection factor $\varepsilon = 0.5$ during isolation and lockdown, and the transmission rates are reduced to $\beta_y' = \beta_y/5 = 0.156$ and $\beta_o' = \beta_o/5 = 0.179$, with $R_0 = 0.9239$ (a), and $\beta_y' = \beta_y/3 = 0.26$ and $\beta_o' = \beta_o/3 = 0.299$, with $R_0 = 1.5398$ (b).

Let us define the reduction in transmission rates among isolated and subsequent locked-down persons. Among them the transmission rates can be reduced by isolating factor ϖ, that is, they are reduced by $\beta_y' = \beta_y/\varpi$ and $\beta_o' = \beta_o/\varpi$, and by protection actions factor ε, that is, $\beta_y' = \varepsilon\beta_y$ and $\beta_o' = \varepsilon\beta_o$, remembering that $\beta_y = 0.78$ and $\beta_o = 0.897$ (both in $days^{-1}$), with $R_0 = 9.239$. Table 5 shows the values attained on May 24 for different factors of reduction in the transmission rates. With respect to $\varpi = 1$ and $\varepsilon = 1$ (first row), D_{2j}, $j = y, o$, and $D_2 = D_{2y} + D_{2o}$ are the difference between values on May 24 and May 10, that is, the number of new cases during this 14 days of lockdown. For other values of ϖ and ε, ΔD_2 is the subtraction of new cases among locked-down persons on May 24 and the new cases among circulating persons without lockdown. Hence, $-$ and $+$ means advantage or disadvantage of lockdown.

The first row in Table 5 shows the dynamics of circulating persons driven by $R_0 = 9.239$ from February 26 to April 3, and by $R_0 = 4.62$ since April 4, and the effective reproduction number $R_{ef} = 1.334$ on June 1. For all other cases, there is beginning of dynamics of CoViD-19

Table 5: The values attained on May 24 for different factors of reduction in the transmission rates: isolating factor ϖ, that is, $\beta'_y = \beta_y/\varpi$ and $\beta'_o = \beta_o/\varpi$, and protection actions factor ε, that is, $\beta'_y = \varepsilon\beta_y$ and $\beta'_o = \varepsilon\beta_o$, remembering that $\beta_y = 0.78$ and $\beta_o = 0.897$ (both in $days^{-1}$), with $R_0 = 9.239$.

ϖ	ε	R_0	R_{ef}	D_{2y}	D_{2o}	D_2	ΔD_{2y}	ΔD_{2o}	ΔD_2
1	1	4.6195	1.527	9800	8330	17860	–	–	–
2	0.6	2.7717	–	21,780	16,130	37,920	−11,980	−7,800	−20,060
2	0.5	2.3098	–	18,700	13,960	32,660	−8,900	−5,630	−14,800
2	0.4	1.8478	–	15,860	11,950	27,810	−6,060	−3,620	−9,950
3	0.6	1.8478	–	15,860	11,950	27,810	−6,060	−3,620	−9,950
3	0.5	1.5398	–	14,100	10,700	24,790	−4,300	−2,370	−6,930
3	0.4	1.2319	–	12,440	9,510	21,950	−2,640	−1,180	−4,090
5	0.6	1.1087	–	11,800	9,056	20,860	−2,000	−726	−3,000
5	0.5	0.9239	–	10,880	8,394	19,270	−1,080	−64	−1,410
5	0.4	0.7391	–	9,988	7,756	17,740	−188	+574	+120
10	0.6	0.5543	–	9,135	7142	16,280	+665	+1,188	+1,580
10	0.5	0.4620	–	8,721	6,844	15,560	+1,079	+1,486	+2,300
10	0.4	0.3696	–	8,316	6,844	14,870	+1,484	+1,779	+2,990
–	0	0	–	6,777	5,438	12,220	+3,023	+2,892	+5,640

transmission among isolated persons, for this reason $R_{ef} = R_0$ on June 1. Observe that the lockdown lasting for 14 days is advantageous if the values of reduction factors ϖ and ε result in $R_0 < 1$ (from Table 5, near one, $R_0 = 0.9239$, is disadvantageous). We stress that expressive numbers of exposed ($E = 734,000$) and pre-diseased ($D_1 = 87,230$) persons are transferred to isolation with lockdown, which implies that many peoples are getting sick in their home. For instance, from last row, when there is absolutely not transmission, $R_0 = 0$, we have 12,220 new cases among isolated persons, which is exactly the contribution of already infected persons before lockdown. In this case, the avoiding of 5,640 new cases due to lockdown (31.6% of 17,860) is desirable, but may bring troubles about releasing strategies later. However, if there is transmission among isolated persons, for instance last but one row $R_0 = 0.3696$, the number of new cases is 14,870, and the difference 2,990 is 16.7% of 17,860, which increases as R_0 increases. If absence or low intensity of transmission could not be guaranteed, lockdown may bring another trouble besides the increased number of new cases: many elder persons should be infected due to closeness with asymptomatic especially young persons [30].

In Figure 20 we present the new epidemics occurring among isolated persons due to initially isolated plus locked-down persons due to high number of asymptomatic persons locked-down. In Figure 20 we show the curves of D_{2y}, D_{2o} and D_2 among circulating (a) and isolated (b) persons, assuming that among isolated persons $\varpi = 10$ (low transmission) and $\varepsilon = 1$ (without protection).

Let us compare the number of cases without lockdown, the lower curve in Figure 9(a) for all persons, and lockdown. We assumed that there is a low transmission among isolated persons due to lockdown, hence the number of new cases is the sum of circulating and isolated persons since after the introduction of lockdown. In Figure 21 we show the curves of D_{2y}, D_{2o} and

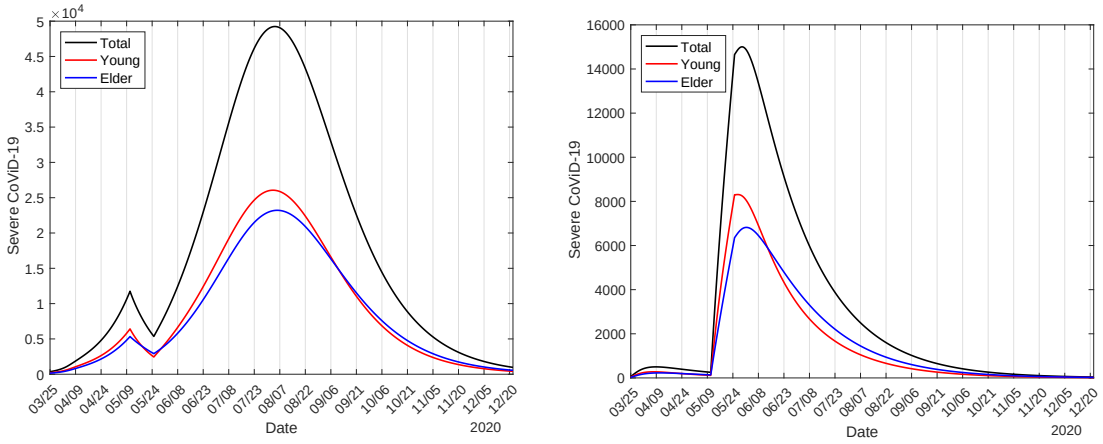

(a) (b)

Figure 20: The curves of D_{2y}, D_{2o}, and D_2 among circulating (a) and isolated (b) persons, assuming that among isolated persons, $\varpi = 10$ (low transmission) and $\varepsilon = 1.0$ (without protection).

D_2 with (continuous) and without (dashed) lockdown for $\varpi = 10$ (low transmission) (a), and $\varpi = 5$ (medium transmission) and (b), assuming $\varepsilon = 1$ for isolated persons. Figure 22(a) is the sum of cases shown in Figure 20. For low transmission, the peaks are $27,280$ (74.72%), $24,780$ (77.44%) and $52,040$ (76.02%) for young, elder and total persons, occurring on August 1, 3, and 2; and for medium transmission, the peaks are $43,760$ (119.86%), $40,270$ (125.84%) and $83,970$ (122.66%), occurring on July 8, 11, and 9. In Figure 21(b), if we assume that isolated persons are using the same protection actions (face mask, hygiene, etc.) of circulating persons $\varepsilon = 0.5$, then the peaks are $25,330$ (69%), $22,700$ (71%) and $48,010$ (70%), occurring on August 14, 16, and 15 (figure not shown). The percentage between parentheses is the ratio between with and without lockdown $D_2(0.9)/D_2(0)$, where $D_2(0)$ for young, elder and total persons are $36,510$, $32,000$, and $68,460$.

Therefore, considering current epidemiological status of São Paulo State, lockdown seems conter-productive if R_0 among isolated persons is relatively high. In this case, suggesting the implementation of lockdown when epidemics is growing rapidly to avoid collapse of health system could not be a good advise. However, lower transmission among isolated persons decreased new cases and moved forward the time of occurrence of peak. Disregarding the intensity of transmission among isolated persons, the implementation of lockdown should be recommended in the beginning, or at most, in the early phase of epidemics.

Until now, we estimated the model parameters to describe the current epidemiological scenario of new coronavirus in São Paulo State. Next, we evaluate the release of isolated persons, which will occur on June 1. Let us summarize the values of epidemiological scenario on June 1 provided by model: S_y, S_o and S are 1.104×10^7 $(43,705\%)$, 1.847×10^6 $(590,095\%)$ and 1.289×10^7 $(50,391\%)$; S_y^{tot}, S_o^{tot} and S^{tot} are 3.09×10^7 $(122,328\%)$, 5.433×10^6 $(1,735,783\%)$ and 3.633×10^7 $(142,025\%)$; I_y, I_o, and I are 3.687×10^6 (10.44%), 0.6903×10^6 (11.3%) and 4.377×10^6 (10.56%); R_{0y}, R_{0o} and R_0 are 3.86, 0.76 and 4.62; and R_{efy}, R_{efo} and R_{ef}

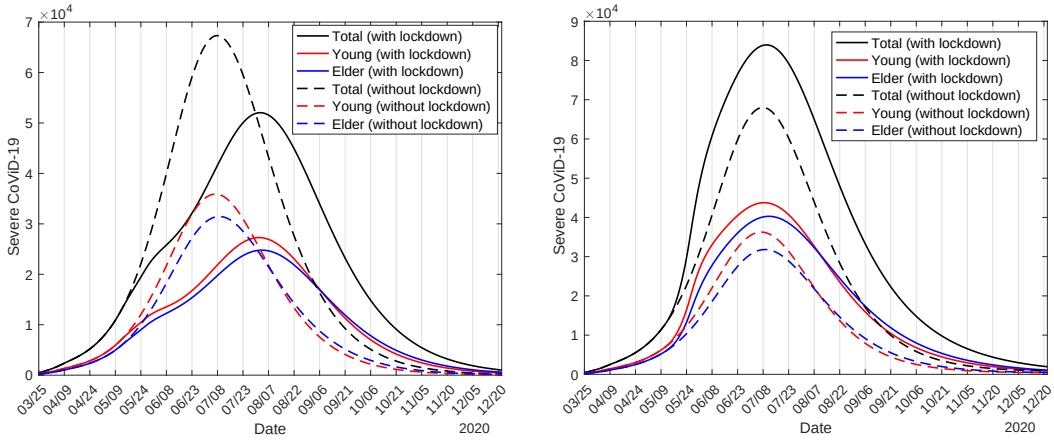

Figure 21: The curves of D_{2y}, D_{2o} and D_2 with (continuous) and without (dashed) lockdown for $\varpi = 10$ (low transmission) (a), and $\varpi = 5$ (medium transmission) and (b), using $\varepsilon = 0.5$ for circulating and $\varepsilon = 1$ for isolated persons.

are 1.1292, 0.205 and 1.334. The percentage between parentheses is the ratio between with ($k = 0.528$ and $\varepsilon = 0.5$) and without ($k = 0$ and $\varepsilon = 1$) interventions for all values. The basic reproduction numbers are those reduced on April 4 due to protection actions ($\varepsilon = 0.5$). There are small number of immune persons (around 0.01% of population), but higher number of susceptible persons (around 78% of population) at the moment of release on June 1, indicating rebounding of epidemics if isolation and protection actions are removed.

3.3 Epidemiological scenarios considering unique isolation followed by releases

In order to obtain epidemiological scenarios, we fix all estimated parameters: the transmission rates $\beta_y = 0.78$ and $\beta_o = 0.897$ (both in $days^{-1}$), giving $R_0 = 9.239$, the mortality rates $\alpha_y = 0.00053$ and $\alpha_o = 0.0053$ (both in $days^{-1}$), the proportion in isolation of susceptible persons $k = 0.528$, and the protection factor $\varepsilon = 0.5$ (reduction in 50%), which reduces the transmission rates to $\beta'_y = 0.39$ and $\beta'_o = 0.4485$ (both in $days^{-1}$), giving $R_0 = 4.62$. Hereafter, all these values are fixed, unless explicitly cited.[3]

The isolation occurred on March 24 will be ended on May 31. We consider three strategies of release, the first beginning on June 1, the second, on June 15, and the third, on June 23. In each strategy, we consider three releases separated by 14 days, with the proportions of release in three consecutive times being l_{1j}, l_{2j} and l_{3j}, for young ($j = y$) and elder ($j = o$) persons.

In strategy A, the releases occur on June 1, 15 and 29, in strategy B, on June 15, 29 and July 13, and in strategy C, on June 23, July 7 and 21 . Remembering that the peaks without release for young, elder and total persons are, respectively, 36, 510, 32, 000, and 68, 460, which occur on June 23, 25 and 23. Hence, in strategy A only the last release occurs after the peak

[3]Simulations were done on May 9-11.

(descending phase of epidemics), in strategy B, only the first peak situates before the peak (ascending phase), and in strategy C, the first release occurs on the peak of epidemics. From Figure 11(a), R_{ef} on June 1, 15 and 23 are, respectively, 1.334, 0.9774 and 0.807.

To obtain the epidemiological scenarios of release, we solve numerically the system of equations (2), (3), and (4) with initial conditions on February 26 given by equation (7), the boundary conditions in isolation occurred on March 24 given by equations (8) and (9), and boundary conditions of releases with first one occurring on June 1 (or 15, or 23) and others, separated by 14 days, given by equations (10) and (11). There is a unique change of parameters in the system of equations, where the transmission rates $\beta_y = 0.78$ and $\beta_o = 0.897$ (both in $days^{-1}$) were reduced to $\beta'_y = 0.39$ and $\beta'_o = 0.4485$ (both in $days^{-1}$) on April 4 due to protection factor $\varepsilon = 0.5$.

Comparing Figures 9(a) and 12, the number of occupied beds follows similar shape of severe CoViD-19 cases D_2. For this reason, we omit the curves of D_2. We evaluate the scheme where isolated population is divided in three equal releases for the strategies A and B, by fixing $l_{1j} = 0.33$, $l_{2j} = 0.5$ and $l_{3j} = 1$, $j = y, o$, and varying protection factor ε.

3.3.1 Strategy A – Release beginning on June 1

In strategy A the releases occur on June 1, 15 and 29. In the first release, $R_{ef} = 1.334$, but the reduced reproduction number R_r given by equation (26) jumps up to higher value than R_{ef} and increased R_{ef} decreases until next release. Hence, at each release time, R_r always increase due to release of susceptible persons.

In Table 6 we show the values and times of occurrence of peaks of D_2, and the numbers of accumulated cases Ω, immune I, cured C and susceptible S persons at the end of the first wave of epidemics, on February 10, 2021, for $\varepsilon = 0.2$, 0.3, 0.4 and 0.5.

Table 6: The values and times of the occurrence of peaks of D_2, and the numbers of accumulated cases Ω, immune I, cured C and susceptible S persons at the end of the first wave of epidemics, on February 10, 2021, for $\varepsilon = 0.2$, 0.3, 0.4 and 0.5. For Strategy A.

	Peak 1	Date	Peak 2	Date	Ω (10^5)	I (10^7)	C (10^5)	S (10^7)
$\varepsilon = 0.5$	217,600	7/17/20	-	-	9.296	4.34	8.682	0.116
$\varepsilon = 0.4$	188,800	7/22/20	-	-	9.101	4.243	8.499	0.213
$\varepsilon = 0.3$	142,600	7/30/20	-	-	8.588	3.992	8.019	0.464
$\varepsilon = 0.2$	57,740	6/12/20	74,520	8/8/20	7.005	3.234	6.535	1.219

We observe the appearing of higher second peak for $\varepsilon = 0.2$, which is due to decreased transmission rates, but insufficient to avoid a small rebounding when susceptible persons are released. The second peak is the original peak being moved forward.

We calculated the number of beds occupied by hospitalized persons using equations (16), (17) and (18), and the number of deaths due to CoViD-19 using equations (20), (21) and (22).

Firstly, we present strategy A with the same protection factor $\varepsilon = 0.5$ in isolation is maintained after release ($\beta'_y = 0.39$ and $\beta'_o = 0.4485$ (both in $days^{-1}$), giving $R_0 = 4.62$). Figure 22 shows the number of occupied beds due to CoViD-19 by young ($j = y$) (a) and elder ($j = o$) (b) for inpatients (B_{1j}), ICU (B_{2j}) and ICU/intubated (B_{3j}) persons.

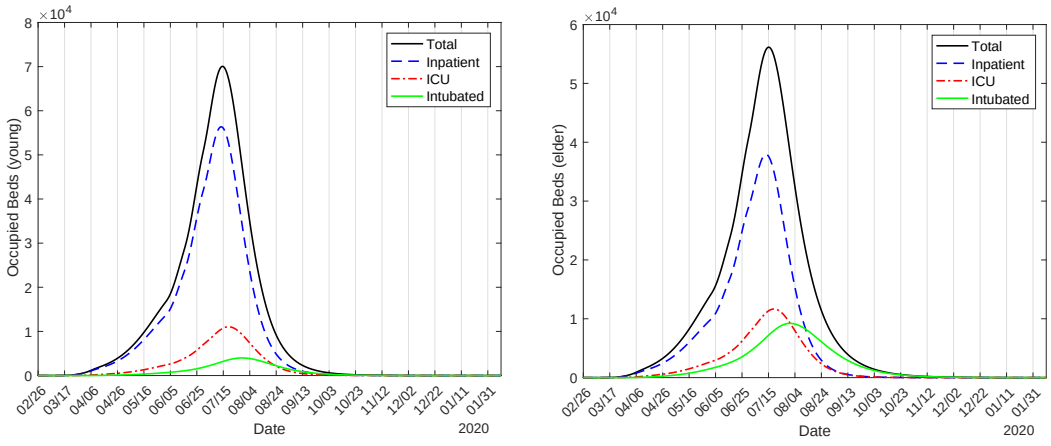

(a) (b)

Figure 22: The number of occupied beds due to CoViD-19 by young ($j = y$) (a) and elder ($j = o$) (b) for inpatients (B_{1j}), ICU (B_{2j}) and ICU/intubated (B_{3j}) persons. Strategy A with $\varepsilon = 0.5$, release beginninng on June 1.

The peak of numbers of occupied beds for young inpatient, ICU, ICU/intubated and total persons are, respectively, 56, 360, 11, 050, 3, 987 and 70, 050, which occur on July 13, 18, 29 and 14. For elder persons, we have, respectively, 37, 940, 11, 660, 9, 215 and 56, 150, which occur on July 13, 19, 31 and 15. The peak of all occupied beds, 126, 200, is 58% of the peak of severe CoViD-19 cases, 217, 600.

Figure 23 shows the number of deaths due to CoViD-19 by young ($j = y$) (a) and elder ($j = o$) (b) for inpatient (Π_{1j}), ICU (Π_{2j}) and ICU/intubated (Π_{3j}) persons. At the end of the first wave of epidemics, the numbers of deaths for young persons occurred in hospital, ICU, ICU/intubated and total are, respectively, 5, 930, 4, 446, 2, 666 and 13, 040. For elder persons, we have, respectively, 16, 820, 12, 610, 11, 760 and 41, 200.

Now, we present strategy A with reduced protection factor $\varepsilon = 0.2$ adopted by all circulating persons after release ($\beta'_y = 0.156$ and $\beta'_o = 0.1794$ (both in $days^{-1}$), giving $R_0 = 1.848$). Figure 24 shows the number of occupied beds due to CoViD-19 by young ($j = y$) (a) and elder ($j = o$) (b) for inpatients (B_{1j}), ICU (B_{2j}) and ICU/intubated (B_{3j}) persons.

The peak of numbers of occupied beds for young inpatient, ICU, ICU/intubated and total persons are, respectively, 16, 680, 3, 450, 1, 412 and 21, 410, which occur on August 1, 7, 22 and 3. For elder persons, we have, respectively, 12, 070, 3, 947, 3, 697 and 19, 390, which occur on August 4, 8, 23 and 4. The peak of all occupied beds, 40, 800, is 54.75% of the peak of severe CoViD-19 cases, 74, 520.

Figure 25 shows the number of deaths due to CoViD-19 by young ($j = y$) (a) and elder ($j = o$) (b) for inpatient (Π_{1j}), ICU (Π_{2j}) and ICU/intubated (Π_{3j}) persons. At the end of the first wave of epidemics, the numbers of deaths for young persons occurred in hospital, ICU, ICU/intubated and total are, respectively, 4, 379, 3, 282, 1, 963 and 9, 625. For elder persons, we have, respectively, 13, 110, 9, 825, 9, 128 and 32, 070. The total number of deaths is 76.9% of protection $\varepsilon = 0.5$.

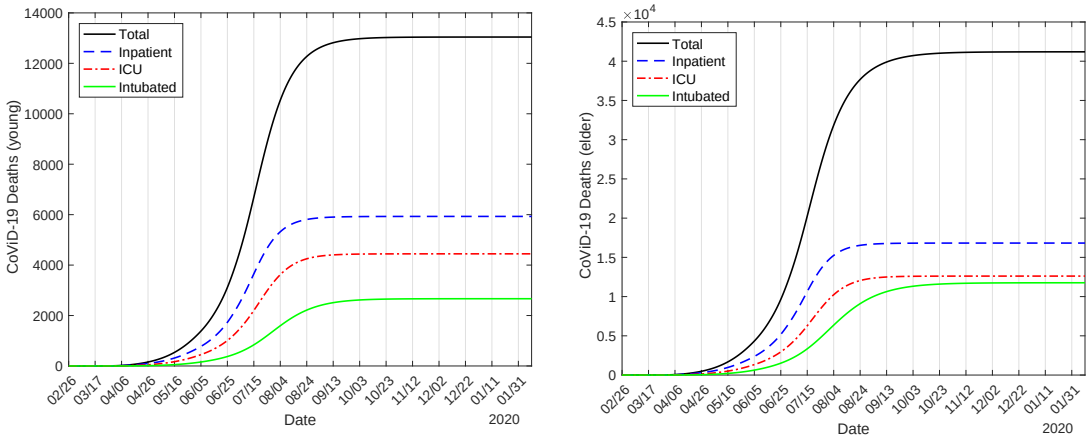

(a) (b)

Figure 23: The number of deaths due to CoViD-19 by young ($j = y$) (a) and elder ($j = o$) (b) for inpatient (Π_{1j}), ICU (Π_{2j}) and ICU/intubated (Π_{3j}) persons. Strategy A with $\varepsilon = 0.5$, release beginninng on June 1.

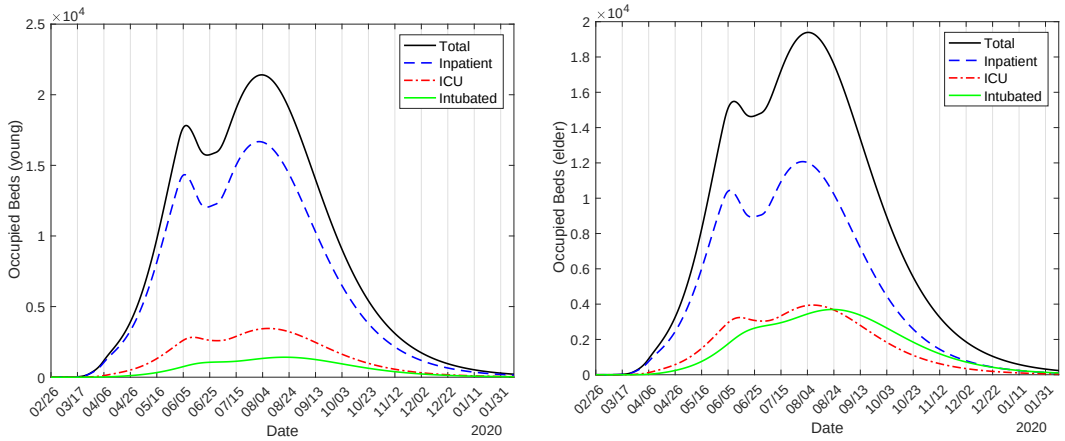

(a) (b)

Figure 24: The number of occupied beds due to CoViD-19 by young ($j = y$) (a) and elder ($j = o$) (b) for inpatients (B_{1j}), ICU (B_{2j}) and ICU/intubated (B_{3j}) persons. Strategy A with $\varepsilon = 0.2$, release beginninng on June 1.

From Table 6 and Figures 22 and 24, we observe that the decreasing in transmission rates due to increased protection actions (factor ε is decreased) becomes the epidemiological scenarios with releases less harmful, decreasing to around 77% when ε decreases from 0.5 to 0.2. Lower ε decreases the transmission rates, and the reduced reproduction number R_{ef} is decreased. The question is: what kind and how intensity protection actions must be adopted by population to decrease the force of infection.

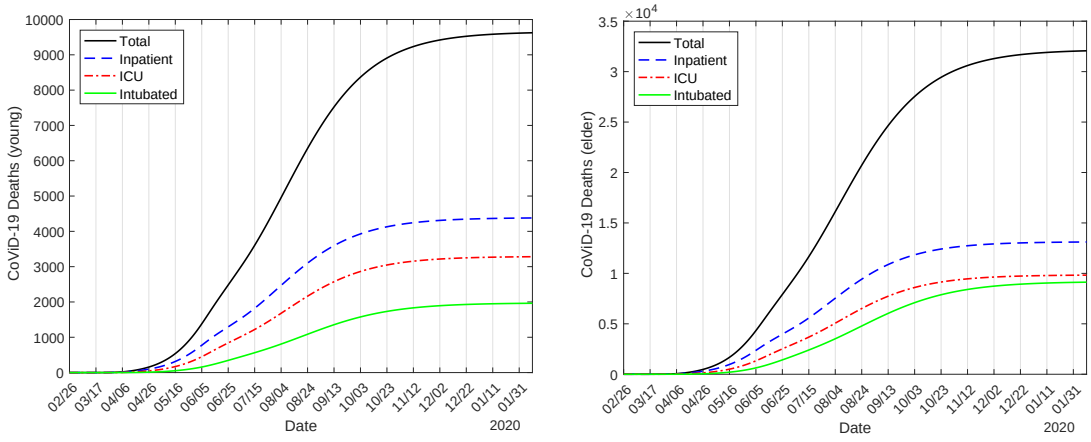

(a) (b)

Figure 25: The number of deaths due to CoViD-19 by young ($j = y$) (a) and elder ($j = o$) (b) for inpatient (Π_{1j}), ICU (Π_{2j}) and ICU/intubated (Π_{3j}) persons. Strategy A with $\varepsilon = 0.2$, release beginninng on June 1.

3.3.2 Strategy B – Release beginning on June 15

In strategy B the releases occur on June 15, 29 and July 13. In the first release, $R_{ef} = 0.9774$, showing a better epidemiological scenario for release than strategy A.

In Table 7 we show the values and times of occurrence of peaks of D_2, and the numbers of accumulated cases Ω, immune I, cured C and susceptible S persons at the end of the first wave of epidemics, on February 10, for $\varepsilon = 0.2$, 0.3, 0.4 and 0.5.

Table 7: The values and times of the occurrence of peaks of D_2, and the numbers of accumulated cases Ω, immune I, cured C and susceptible S persons at the end of the first wave of epidemics, on February 10, 2021, for $\varepsilon = 0.2$, 0.3, 0.4 and 0.5. For Strategy B.

	Peak 1	Date	Peak 2	Date	Ω (10^5)	I (10^7)	C (10^5)	S (10^7)
$\varepsilon = 0.5$	185,900	8/2/20	-	-	9.247	4.318	8.638	0.139
$\varepsilon = 0.4$	158,500	8/6/20	-	-	9.016	4.203	8.422	0.253
$\varepsilon = 0.3$	116,400	8/12/20	-	-	8.439	3.922	7.881	0.534
$\varepsilon = 0.2$	67,290	6/20/20	59,540	8/4/20	6.773	3.124	6.316	1.325

We present the number of beds occupied by hospitalized persons using equations (16), (17) and (18). We calculate the number of deaths due to CoViD-19 using equations (20), (21) and (22).

Firstly, we present strategy B with the same protection factor $\varepsilon = 0.5$ in isolation is maintained after release ($\beta'_y = 0.39$ and $\beta'_o = 0.4485$ (both in $days^{-1}$), giving $R_0 = 4.62$). Figure 26 shows the number of occupied beds due to CoViD-19 by young ($j = y$) (a) and elder ($j = o$) (b) for inpatients (B_{1j}), ICU (B_{2j}) and ICU/intubated (B_{3j}) persons.

The peak of numbers of occupied beds for young inpatient, ICU, ICU/intubated and total

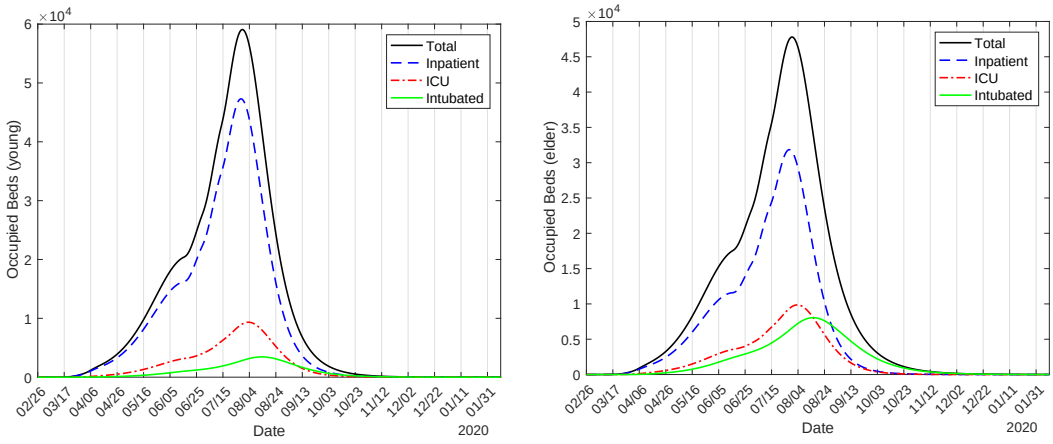

(a) (b)

Figure 26: The number of occupied beds due to CoViD-19 by young ($j = y$) (a) and elder ($j = o$) (b) for inpatients (B_{1j}), ICU (B_{2j}) and ICU/intubated (B_{3j}) persons. Strategy B with $\varepsilon = 0.5$, release beginninng on June 15.

persons are, respectively, 47, 290, 9, 335, 3, 446 and 59, 070, which occur on July 28, August 3, 13 and July 29. For elder persons, we have, respectively, 31, 850, 9, 858, 8050 and 47, 790, which occur on July 28, August 3, 15 and July 30. The peak of all occupied beds, 106, 860, is 57.48% of the peak of severe CoViD-19 cases, 185, 900, and this peak of all occupied beds is 85% of the peak observed in strategy A.

Figure 27 shows the number of deaths due to CoViD-19 by young ($j = y$) (a) and elder ($j = o$) (b) for inpatient (Π_{1j}), ICU (Π_{2j}) and ICU/intubated (Π_{3j}) persons. At the end of the first wave of epidemics, the numbers of deaths for young persons occurred in hospital, ICU, ICU/intubated and total are, respectively, 5, 896, 4, 421, 2, 651 and 12, 970. For elder persons, we have, respectively, 16, 750, 12, 560, 11, 710 and 41, 010. The total number of deaths is 99.5% of strategy A.

Now, we present strategy B with reduced protection factor $\varepsilon = 0.2$ adopted by all circulating persons after release ($\beta'_y = 0.156$ and $\beta'_o = 0.1794$ (both in $days^{-1}$), giving $R_0 = 1.8478$). Figure 28 shows the number of occupied beds due to CoViD-19 by young ($j = y$) (a) and elder ($j = o$) (b) for inpatients (B_{1j}), ICU (B_{2j}) and ICU/intubated (B_{3j}) persons.

The peak of numbers of occupied beds for young inpatient, ICU, ICU/intubated and total persons are, respectively, 16, 240, 3, 271, 1, 234 and 20, 480, which occur on June 16, 21, July 2 and June 17. For elder persons, we have, respectively, 11, 590, 3, 682, 3, 091 and 17, 680, which occur on June 16, 21, July 7 and June 18 . The peak of all occupied beds, 38, 160, is 56.7% of the peak of severe CoViD-19 cases, 67, 290, and this peak of all occupied beds is 93% of the peak observed in strategy A.

Figure 29 shows the number of deaths due to CoViD-19 by young ($j = y$) (a) and elder ($j = o$) (b) for inpatient (Π_{1j}), ICU (Π_{2j}) and ICU/intubated (Π_{3j}) persons. At the end of the first wave of epidemics, the numbers of deaths for young persons occurred in hospital, ICU, ICU/intubated and total are, respectively, 4, 233, 3, 171, 1, 894 and 9, 298. For elder persons,

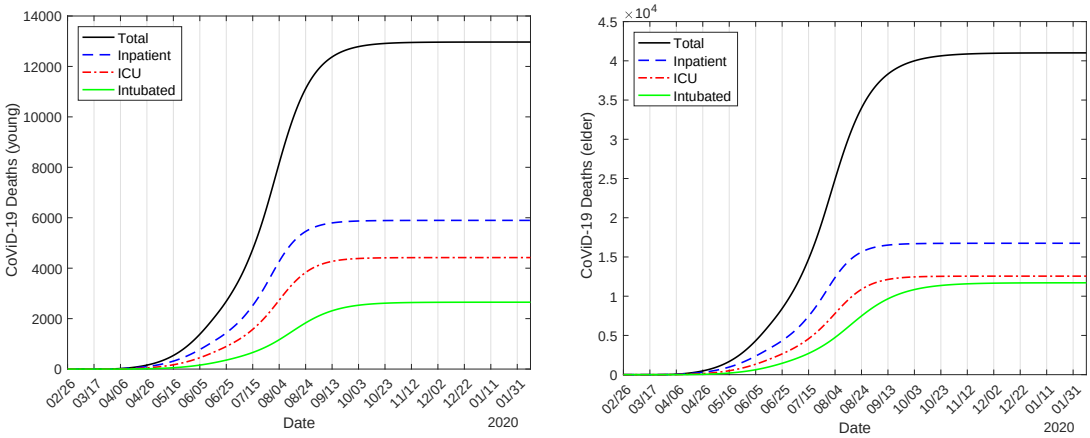

Figure 27: The number of deaths due to CoViD-19 by young ($j = y$) (a) and elder ($j = o$) (b) for inpatient (Π_{1j}), ICU (Π_{2j}) and ICU/intubated (Π_{3j}) persons. Strategy B with $\varepsilon = 0.5$, release beginning on June 15.

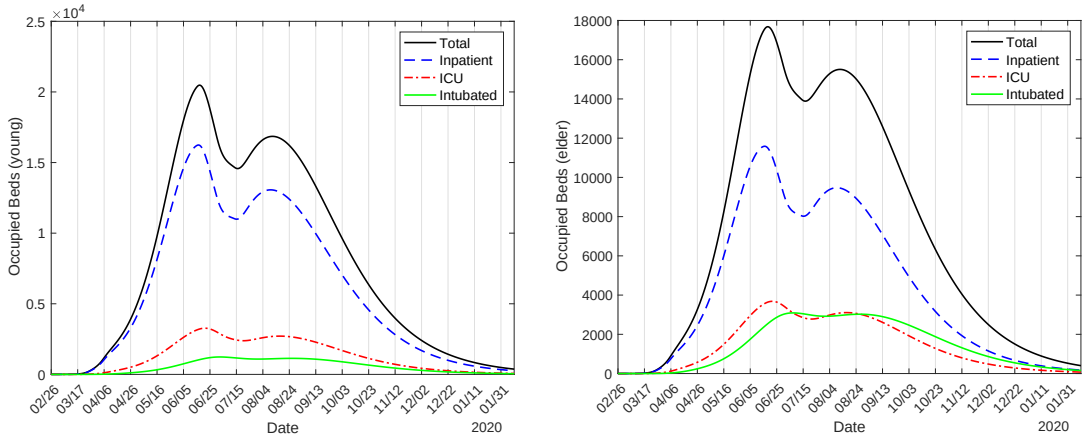

Figure 28: The number of occupied beds due to CoViD-19 by young ($j = y$) (a) and elder ($j = o$) (b) for inpatients (B_{1j}), ICU (B_{2j}) and ICU/intubated (B_{3j}) persons. Strategy B with $\varepsilon = 0.2$, release beginninng on June 15.

we have, respectively, 12,670, 9,491, 8,798 and 30,960. The total number of deaths is 74.6% of protection $\varepsilon = 0.5$, and 96.5% of strategy A.

From Figures 26 and 28, we observe quite similar behavior observed in Figures 22 and 24, strategy A, except the second peak is lower than the first. The number of deaths decreased to around 75% when ε decreases from 0.5 to 0.2, while in comparison with strategy A, very small decreasing to around 95%.

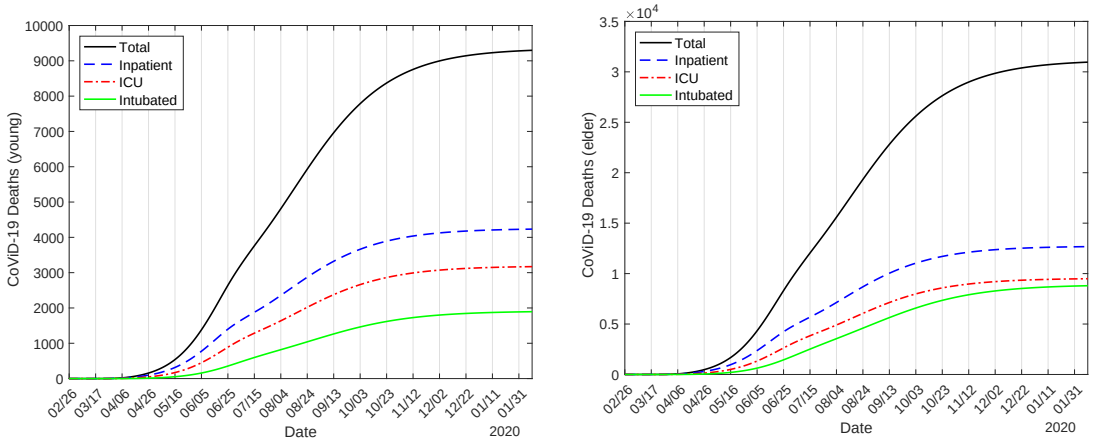

(a) (b)

Figure 29: The number of deaths due to CoViD-19 by young ($j = y$) (a) and elder ($j = o$) (b) for inpatient (Π_{1j}), ICU (Π_{2j}) and ICU/intubated (Π_{3j}) persons. Strategy B with $\varepsilon = 0.2$, release beginninng on June 15.

3.3.3 Strategy C – Release beginning on June 23

In strategy B the releases occur on June 23, July 7 and 21. In the first release, $R_{ef} = 0.807$, showing a better epidemiological scenario than strategies A and B. Remember that June 24 is the peak of the epidemics.

In Table 8 we show the values and times of occurrence of peaks of D_2, and the numbers of accumulated cases Ω, immune I, cured C and susceptible S persons at the end of the first wave of epidemics, on April 1, for $\varepsilon = 0.2$, 0.3, 0.4 and 0.5.

Table 8: The values and times of the occurrence of peaks of D_2, and the numbers of accumulated cases Ω, immune I, cured C and susceptible S persons at the end of the first wave of epidemics, on February 10, 2021, for $\varepsilon = 0.2$, 0.3, 0.4 and 0.5. For Strategy C.

	Peak 1	Date	Peak 2	Date	Ω (10^5)	I (10^7)	C (10^5)	S (10^7)
$\varepsilon = 0.5$	170, 100	8/12/20	-	-	9.218	4.297	8.597	0.1598
$\varepsilon = 0.4$	142, 700	8/16/20	-	-	8.963	4.171	8.359	0.286
$\varepsilon = 0.3$	68, 460	6/24/20	102, 000	8/23/20	8.344	3.871	7.78	0.586
$\varepsilon = 0.2$	68, 450	6/23/20	50, 290	8/20/20	6.631	3.057	6.177	1.397

We present the number of beds occupied by hospitalized persons using equations (16), (17) and (18). We calculate the number of deaths due to CoViD-19 using equations (20), (21) and (22).

Firstly, we present strategy B with the same protection factor $\varepsilon = 0.5$ in isolation is maintained after release ($\beta'_y = 0.39$ and $\beta'_o = 0.4485$ (both in $days^{-1}$), giving $R_0 = 4.62$). Figure 30 shows the number of occupied beds due to CoViD-19 by young ($j = y$) (a) and elder ($j = o$) (b) for inpatients (B_{1j}), ICU (B_{2j}) and ICU/intubated (B_{3j}) persons.

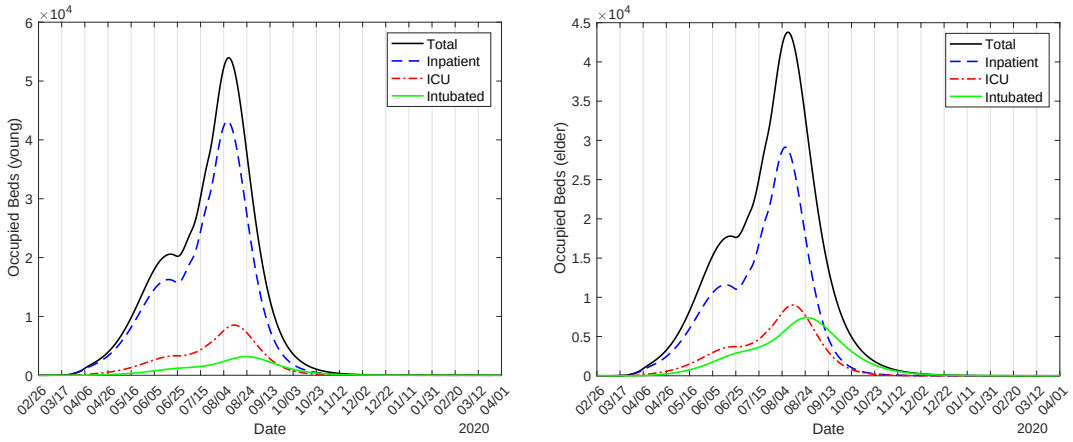

(a) (b)

Figure 30: The number of occupied beds due to CoViD-19 by young ($j = y$) (a) and elder ($j = o$) (b) for inpatients (B_{1j}), ICU (B_{2j}) and ICU/intubated (B_{3j}) persons. Strategy C with $\varepsilon = 0.5$, release beginninng on June 23.

The peak of numbers of occupied beds for young inpatient, ICU, ICU/intubated and total persons are, respectively, 43,180, 8,528, 3,163 and 53,950, which occur on August 7, 12, 23 and 8. For elder persons, we have, respectively, 29,130, 9,017, 7,418 and 43,780, which occur on August 7, 13, 25 and 8. The peak of all occupied beds, 97,730, is 57.45% of the peak of severe CoViD-19 cases, 170,100, and this peak of all occupied beds is 77.44% and 91.46% of the peaks observed in strategies A and B, respectively.

Figure 31 shows the number of deaths due to CoViD-19 by young ($j = y$) (a) and elder ($j = o$) (b) for inpatient (Π_{1j}), ICU (Π_{2j}) and ICU/intubated (Π_{3j}) persons. At the end of the first wave of epidemics, the numbers of deaths for young persons occurred in hospital, ICU, ICU/intubated and total are, respectively, 5,876, 4,406, 2,642 and 12,920. For elder persons, we have, respectively, 16,700, 12,520, 11,680 and 40,900. The total number of deaths is 99.2% and 99.7% of, respectively, strategies A and B.

Now, we present strategy C with reduced protection factor $\varepsilon = 0.2$ adopted by all circulating persons after release ($\beta'_y = 0.156$ and $\beta'_o = 0.1794$ (both in $days^{-1}$), giving $R_0 = 1.8478$). Figure 32 shows the number of occupied beds due to CoViD-19 by young ($j = y$) (a) and elder ($j = o$) (b) for inpatients (B_{1j}), ICU (B_{2j}) and ICU/intubated (B_{3j}) persons.

The peak of numbers of occupied beds for young inpatient, ICU, ICU/intubated and total persons are, respectively, 16,260, 3,312, 1,273 and 20,570, which occur on June 17, 24, July 5 and June 18. For elder persons, we have, respectively, 11,590, 3,714, 3,168 and 17,790, which occur on June 16, 24, July 7 and June 21 . The peak of all occupied beds, 38,360, is 56.04% of the peak of severe CoViD-19 cases, 68,450, and this peak of all occupied beds is 94% and 100.5% of the peaks observed in strategies A and B, respectively.

Figure 33 shows the number of deaths due to CoViD-19 by young ($j = y$) (a) and elder ($j = o$) (b) for inpatient (Π_{1j}), ICU (Π_{2j}) and ICU/intubated (Π_{3j}) persons. At the end of the first wave of epidemics, the numbers of deaths for young persons occurred in hospital, ICU,

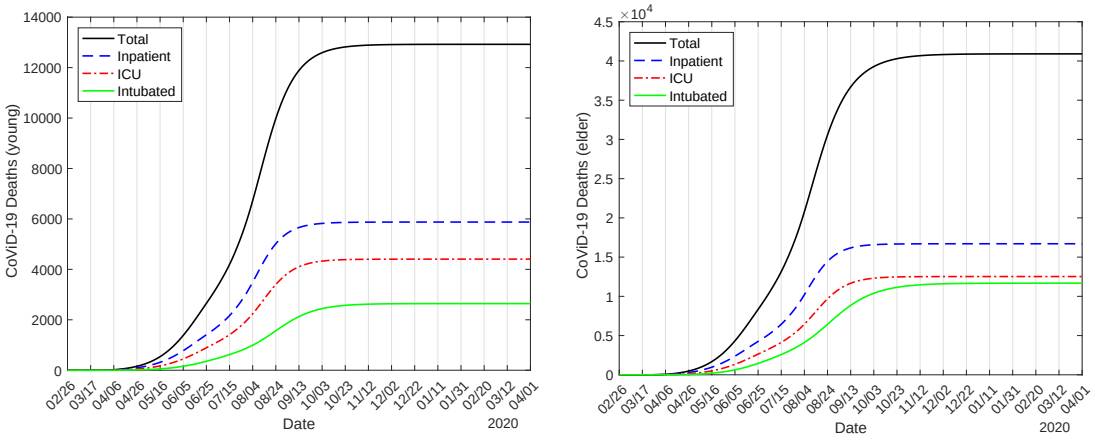

(a) (b)

Figure 31: The number of deaths due to CoViD-19 by young ($j = y$) (a) and elder ($j = o$) (b) for inpatient (Π_{1j}), ICU (Π_{2j}) and ICU/intubated (Π_{3j}) persons. Strategy C with $\varepsilon = 0.5$, release beginninng on June 23.

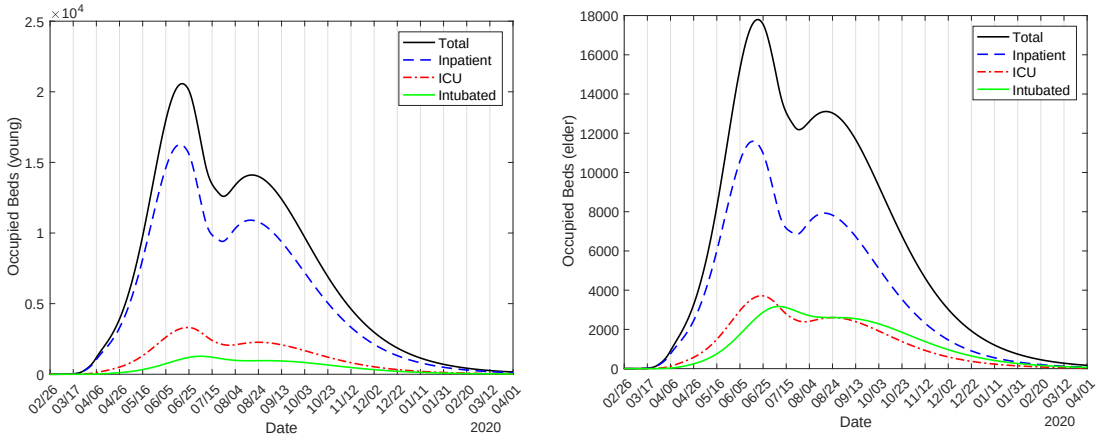

(a) (b)

Figure 32: The number of occupied beds due to CoViD-19 by young ($j = y$) (a) and elder ($j = o$) (b) for inpatients (B_{1j}), ICU (B_{2j}) and ICU/intubated (B_{3j}) persons. Strategy C with $\varepsilon = 0.2$, release beginninng on June 23.

ICU/intubated and total are, respectively, $4,147$, $3,108$, $1,861$ and $9,115$. For elder persons, we have, respectively, $12,410$, $9,298$, $8,650$ and $30,350$. The total number of deaths is 73.3% of protection $\varepsilon = 0.5$, and 94.7% and 96.5% of, respectively, strategies A and B.

From Figures 30 and 32, we observe quite similar behavior observed in Figures 26 and 28, strategy B, except the first lower peak appears earlier. The number of deaths decreased to around 74% when ε decreases from 0.5 to 0.2, while in comparison with strategies A and B, very small decreasing to around 95%. The little difference in the number of deaths in strategies

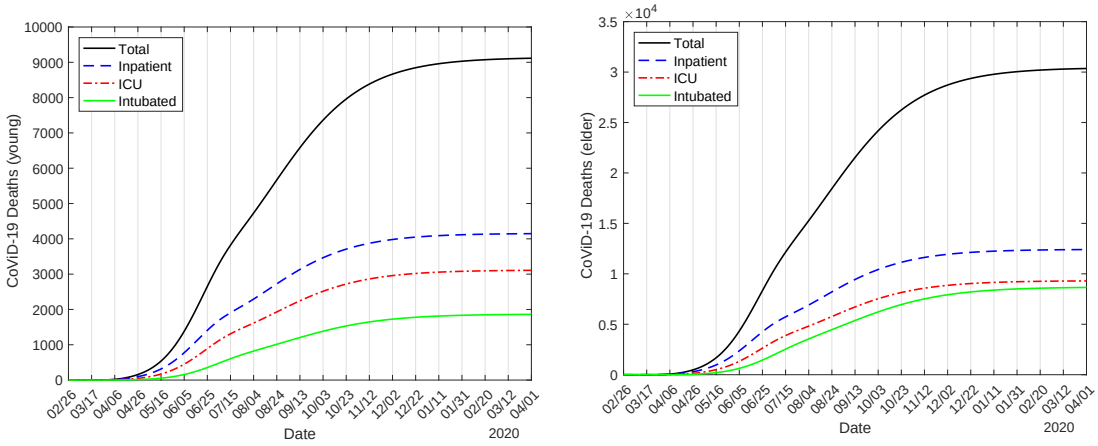

(a) (b)

Figure 33: The number of deaths due to CoViD-19 by young ($j = y$) (a) and elder ($j = o$) (b) for inpatient (Π_{1j}), ICU (Π_{2j}) and ICU/intubated (Π_{3j}) persons. Strategy C with $\varepsilon = 0.2$, release beginninng on June 23.

A, B and C can be explained by R_{ef} situating around one at the time of the first release.

4 Discussion

The system of equations (2), (3), and (4) is simulated to provide epidemiological scenarios using parameters estimated from data collected in São Paulo State [3] from February 26 to May 7, 2020 (see Figure 2). Based on those data, we estimated the transmission rates $\beta_y = 0.78$ and $\beta_o = 0.897$ (both in $days^{-1}$), giving $R_0 = 9.239$ (partials $R_{0y} = 7.725$ and $R_{0o} = 1.514$), and the fatality rates $\alpha_y = 0.00053$ and $\alpha_o = 0.0053$ (both in $days^{-1}$). Isolation was introduced on March 24, hence, we estimated the proportion in isolation of susceptible persons $k = 0.528$, which was the average proportion of daily proportions observed in São Paulo State from February 26 to May 3. Nevertheless, the observed data suggested an additional protection, and we estimated this protection as $\varepsilon = 0.5$ since April 4, which reduces the transmission rates to $\beta'_y = 0.39$ and $\beta'_o = 0.4485$ (both in $days^{-1}$), giving $R_0 = 4.62$. Hence, from February 26 to April 3, the epidemics was driven by force of infection with $R_0 = 9.239$, and since April 4, by force of infection with $R_0 = 4.62$, however at each time R_{ef} determines the number of new cases.

In [30] and [31] we estimated the additional mortality rates based on the observed data, and concluded that their values did not provide log-term reliable values. For instance, this estimation resulted in 30% up to 80% of deaths of all severe CoViD-19 cases. For this reason, we estimated considering final deaths to be around 10% of elder persons, disregarding the observed data. Here, we concluded that the observed data must be taken into account, however delayed 9 days (fatality rates) or 15 days (fatality proportions).

Instead daily collected CoViD-199 data, we used the accumulated data to estimate model parameters (see Figures 3, 4, 6 and 8) using Ω given by equation (13), and retrieved the curve

of severe CoViD-19 D_2, indicating that the peak reaches $68,460$ on June 23, and at this day, accumulated cases Ω is $243,000$. Using those estimated parameters, we retrieved daily cases of CoViD-19 (see Figure 16) using Ω_d given by equation (15), indicating that on June 12 the peak reaches $5,287$ cases.

We evaluated the current epidemiological scenario in São Paulo State with proportion in isolation $k = 0.528$ and protection $\varepsilon = 0.5$, which decreased the basic reproduction number to $R_0 = 4.62$. This value is higher than the estimation provided by simple SIR model, providing around $R_0 = 2.5$. Based on the new severe CoViD-19 cases, we estimated the occupancy of beds in hospital and deaths (see Figures 13 and 14). On June 1, the time of release, the total number of deaths is around $8,500$ (see Table 4). We also estimated the ratio hidden:apparent cases of new coronavirus as epidemics evolves (see Figures 17 and 18), suggesting around 25 asymptomatic cases by one symptomatic person.

We also observed potential risk of interdicting lockdown due to current epidemiological status. When hypothetically transmission occurs in non-interacting young and elder subpopulations, in long-term epidemics, they reach $s_y^{is*} = 1/R_{0y} = 0.13$ and $s_o^{is*} = 1/R_{0o} = 0.66$. However, from numerical simulations without releasing, we obtained $s_y^* = 0.1034$ and $s_o^* = 0.0017$ when these subpopulations are interacting. Notice that the difference $s_y^{is*} - s_y^*$ is the additional proportion of susceptible persons infected due to interaction, being 2.7% for young and 66% for elder persons, showing that elder persons are 24.4-times more risk than young persons when interacting. For this reason, if lockdown is implemented, assuming that there is low transmission (through restricted contact occurring in the household and/or neighborhood) among isolated persons due to asymptomatic persons locked-down, elder persons are under more risk, and consequently, deaths can increase.

We studied possible scenarios of releasing in considering three different times for the first release, the strategies A (first release on June 1, with $R_{ef} = 1.334$), B (first release on June 15, with $R_{ef} = 0.9774$) and C (first release on June 1, with $R_{ef} = 0.807$). The approximated effective reproduction number R_{ef} was calculated by equation (24). We observed that increase in protection actions can manage the epidemics in terms of available hospital beds and deaths, which decreased 75% when ε is decreased from 0.5 to 0.2. Maybe the massive educational campaign can achieve the goal by increasing the protection actions, that is, decreasing ε for at least 0.2. However, the three strategies presented very little difference (around 5%) with respect to delaying the time of release. This is result of R_{ef} being close to one.

Model parameters were estimated to describe the isolation and protection actions affecting on current epidemiological status, and subsequent release. However, from Figure 7(a), we observed a lowering in severe CoViD-19 data with respect to the estimated curve. However, more data must be considered to decide it this is a tendency or not due to new coronavirus being irradiated to small cities from São Paulo City.

5 Conclusion

We formulated a mathematical model considering two subpopulations comprised by young and elder persons to study CoViD-19 in São Paulo State, Brazil. The model considering pulses in isolation and release was simulated to describe current epidemiological status in São Paulo

State and future scenarios when releases will occur on June 1.

Isolation as well as lockdown are valuable measures to control epidemics with high lethality. However, lockdown with short period of time could not be an appropriate control efforts if epidemics is in ascending phase, and there is non-negligible transmission among isolated persons. The transferring of elevated number of asymptomatic persons by lockdown to isolation may trigger a new epidemics among originally isolated persons. A false feeling of absence of transmission among isolated persons could be prevailed due to the lower initial estimation of the basic reproduction number, around $R_0 = 2.5$. However, our model estimated $R_0 = 9.239$, which may increase the possibility of transmission among isolated persons due to airborne transmission.

From the epidemiological scenarios of release, we observed that the delay to implement the release (June 1, 15 and 24) affected very little, reduction in around 5%. in the number of occupancy of beds and deaths. The effective reproduction number R_{ef} in these three strategies is around 1, hence postponing the release of isolated persons when R_{ef} decreases more could be better strategy. However, the increased in protection actions, reducing ε from 0.5 to 0.2 reduced in around 15% the occupancy of beds and deaths. Hence, release beginning on June 1 accompanied by massive educational campaign could the implemented.

Finally, severe CoViD-19 data collected in the São Paulo State indicates that there is another lowering in those cases besides the diminishing resulted from isolation and protection. We hypothesized that this decreasing could be due to spreading of new coronavirus to small cities irradiated from São Paulo City, which changes in demography (population density), but more data are needed to confirm or deny this hypothesis. The model considered homogeneous space (population density) and time (constant parameters) in São Paulo State. However, this model can be applied to cities taking into account their population densities, for instance. Notice that considering 44.6 million of inhabitants and $R_0 = 9.239$ in São Paulo State, the epidemics will be established strongly due to the threshold to trigger epidemics is very low, $N^{th} = 4.83$ million of persons.

References

[1] Adesão ao isolamento social em SP (April 27, 2020). https://www.saopaulo.sp.gov.br/coronavirus/isolamento.

[2] M.M. Arons, *et al.*, Presymptomatic SARS-CoV-2 infections and transmission in a skilled nursing facility, The New Engl. Jour. Medicine (2020) April 24, DOI: 10.1056/NEJMoa2008457.

[3] Casos em São Paulo (April 30, 2020). https://www.saopaulo.sp.gov.br/coronavirus#numero-vacinacao.

[4] R.M. Anderson, R.M. May, R.M., Infectious Diseases of Human. Dynamics and Control, Oxford University Press, Oxford, New York, Tokyo (1991).

[5] J.A. Backer, D. Klinkenberg, J. Wallinga, Incubation period of 2019 novel coronavirus (2019-nCoV) infections among travellers from Wuhan, China, 20-28 Jan-

uary 2020, Euro Surveill. (2020) 25(5) pii=2000062. https://doi.org/10.2807/1560-7917.ES.2020.25.5.2000062

[6] Boletim Epidemiológico 08 (April 9, 2020), https://www.saude.gov.br/images/pdf/2020/April/09/be-covid-08-final-2.pdf.

[7] O. Diekmann, J.A.P. Heesterbeek, M.G. Roberts, The construction of next-generation matrices for compartmental epidemic models, J. R. Soc. Interface 7 (2010) 873-885.

[8] N.M. Ferguson, *et al.*, Impact of non-pharmaceutical interventions (NPIs) to reduce COVID-19 mortality and healthcare demand, Imperial College COVID-19 Response Team (2020).

[9] J. Howad, *et al.*, Face masks against COVID-19: An evidence review, (April 12, 2020), doi:10.20944/preprints202004.0203.v1.

[10] Info.Gripe – Fiocurz (April 28, 2020), http://info.gripe.fiocruz.br/.

[11] K. McIntosh, M.S. Hirsch, A. Bloom, Coronavirus disease 2019 (COVID-19): Epidemiology, virology, clinical features, diagnosis, and prevention, UpToDate (April 30, 2020). https://www.uptodate.com/contents/coronavirus-disease-2019-covid-19-epidemiology-virology-clinical-features-diagnosis-and-prevention/print.

[12] L. Qun, *et.al.*, Early transmission dynamics in Wuhan, China, of Novel Coronavirus-Infected Pneumonia, The New Engl. J. Medicine 182(13) (2020) 1199-1207.

[13] S.M. Raimundo, H.M. Yang, R.C. Bassanezi, M.A.C. Ferreira, The attracting basins and the assessment of the transmission coefficients for HIV and *M. tuberculosis* infections among women inmates, Journal of Biological Systems (10)(1) (2002) 61-83.

[14] SEADE – Fundação Sistema Estadual, https://www.seade.gov.br (2020).

[15] Z. Shuai, P. van den Driessche, Global stability of infectious disease model using Lyapunov functions, SIAM J. App. Math. 73(4) (2013) 1513-1532.

[16] The Novel Coronavirus Pneumonia Emergency Response Epidemiology Team, The epidemiological characteristics of an outbreak of 2019 novel coronavirus diseases (COVID-19) – China, 2020, China CDC (released on February 17, 2020).

[17] D. Wang, *et al.*, Clinical characteristics of 138 hospitalized patients with 2019 novel coronavirus–infected pneumonia in Wuhan, China, JAMA, 323(11) (2020) 1061-1069.

[18] WHO, Report of the WHO-China Joint Mission on Coronavirus Disease 2019 (COVID-19), 16-24 February 2020 (2020).

[19] H.M. Yang, Modelling vaccination strategy against directly transmitted diseases using a series of pulses, Journal of Biological Systems (6)(2) (1998) 187-212.

[20] H.M. Yang, Directly transmitted infections modeling considering age-structured contact rate – Epidemiological analysis, Mathematical and Computer Modelling 29(7) (1999) 11-30.

[21] H.M. Yang, Directly transmitted infections modeling considering age-structured contact rate, Mathematical and Computer Modelling, 29(8) (1999) 39-48.

[22] H.M. Yang, W.C. Ferreira, A populational model applied to HIV transmission considering protection and treatment, IMA J. Mat. appl. Med. Biol. 16 (1999) 237-259.

[23] H.M. Yang, Modeling directly transmitted infections in a routinely vaccinated population – The force of infection described by Volterra integral equation, Applied Mathematics and Computation (122)(1) (2001) 27-58.

[24] H.M. Yang, The basic reproduction number obtained from Jacobian and next generation matrices – A case study of dengue transmission modelling, BioSystems 126 (2014) 52-75.

[25] H.M. Yang, D. Greenhalgh, Proof of conjecture in: The basic reproduction number obtained from Jacobian and next generation matrices – A case study of dengue transmission modelling, Appl. Math. Comput. 265 (2015) 103-107.

[26] H.M. Yang, J.L. Boldrini, A.C. Fassoni, K.K.B. Lima, L.S.F. Freitas, M.C. Gomez, V.F. Andrade, A.R.R. Freitas, Fitting the incidence data from the City of Campinas, Brazil, based on dengue transmission modellings considering time-dependent entomological parameters, PlosOne (March 24) (2016) 1-41.

[27] H.M. Yang, The transovarial transmission un the dynamics of dengue infection: Epidemiological implications and thresholds, Math. Biosc. 286 (2017) 1-15.

[28] M.C. Gomez, H.M. Yang, A simple mathematical model to describe antibody-dependent enhancement in heterologous secondary infection in dengue, Mathem. Med. Biol.: A Journal of the IMA ?? (2018), 1-28.

[29] H.M. Yang, Are the beginning and ending phases of epidemics provided by next generation matrices? – Revisiting drug sensitive and resistant tuberculosis model, Appl. Math. Comput., submitted (2020).

[30] H.M. Yang, L.P. Lombardi Jr, A.C. Campos, Modeling the transmission of new coronavirus in the São Paulo State, Brazil – Assessing epidemiological impacts of isolating young and elder persons, Mathem. Med. and Biol.: A journal of the IMA, submitted (2020).

[31] H.M. Yang, L.P. Lombardi Jr, F.F.M. Castro, A.C. Campos, Mathematical model describing CoViD-19 in São Paulo State, Brazil – Evaluating isolation as control mechanism and forecasting epidemiological scenarios of release, Epidem. Infect., submitted (2020).

A Trivial equilibrium and its stability

By the fact that N is varying, the system is non-autonomous non-linear differential equations. To obtain autonomous system of equations we let $k_j = l_{ij} = 0$, $j = y, o$, and use fractions of individuals in each compartment, defined by, with $j = y$ and o,

$$x_j = \frac{X_j}{N}, \quad \text{where} \quad X = S_j, Q_j, E_j, A_j, Q_{1_j}, D_{1_j}, Q_{2_j}, D_{2_j}, I,$$

resulting in

$$\frac{d}{dt}x_j \equiv \frac{d}{dt}\frac{X_j}{N} = \frac{1}{N}\frac{d}{dt}X_j - x_j\frac{1}{N}\frac{d}{dt}N = \frac{1}{N}\frac{d}{dt}X_j - x\left(\phi - \mu\right) + x_j\left(\alpha_y d_{2y} + \alpha_o d_{2o}\right),$$

using equation (5) for N. Hence, equations (2), (3) and (4) in terms of fractions become, for susceptible persons,

$$\begin{cases} \frac{d}{dt}s_y &= \phi - \left(\varphi + \phi\right)s_y - \lambda s_y + s_y\left(\alpha_y d_{2y} + \alpha_o d_{2o}\right) \\ \frac{d}{dt}s_o &= \varphi s_y - \phi s_o - \lambda\psi s_o + s_o\left(\alpha_y d_{2y} + \alpha_o d_{2o}\right), \end{cases} \tag{A.1}$$

for infected persons,

$$\begin{cases} \frac{d}{dt}q_j &= -\phi q_j + q_j\left(\alpha_y d_{2y} + \alpha_o d_{2o}\right) \\ \frac{d}{dt}e_j &= \lambda\left(\delta_{jy} + \psi\delta_{jo}\right)s_j - \left(\sigma_j + \phi\right)e_j + e_j\left(\alpha_y d_{2y} + \alpha_o d_{2o}\right) \\ \frac{d}{dt}a_j &= p_j\sigma_j e_j - \left(\gamma_j + \eta_j + \phi\right)a_j + a_j\left(\alpha_y d_{2y} + \alpha_o d_{2o}\right) \\ \frac{d}{dt}d_{1j} &= \left(1 - p_j\right)\sigma_j e_j - \left(\gamma_{1j} + \eta_{1j} + \phi\right)d_{1j} + d_{1j}\left(\alpha_y d_{2y} + \alpha_o d_{2o}\right) \\ \frac{d}{dt}q_{2j} &= \left(1 - \chi_j\right)\gamma_j a_j + m_j\gamma_{1j}d_{1j} + \xi_j q_{3j} - \left(\gamma_{3j} + \eta_{2j} + \varepsilon_{4j} + \phi\right)q_{2j} + q_{2j}\left(\alpha_y d_{2y} + \alpha_o d_{2o}\right) \\ \frac{d}{dt}q_{3j} &= \varepsilon_{4j}q_{2j} - \left(\gamma_{3j} + \xi_j + \phi\right)q_{3j} + q_{3j}\left(\alpha_y d_{2y} + \alpha_o d_{2o}\right) \\ \frac{d}{dt}q_{1j} &= \eta_{1j}d_{1j} - \left(\gamma_{2j} + \gamma_{1j} + \phi\right)q_{1j} + q_{1j}\left(\alpha_y d_{2y} + \alpha_o d_{2o}\right) \\ \frac{d}{dt}d_{2j} &= \left(1 - m_j\right)\gamma_{1j}\left(d_{1j} + q_{1j}\right) - \left(\gamma_{2j} + \theta_j + \phi + \alpha_j\right)d_{2j} + d_{2j}\left(\alpha_y d_{2y} + \alpha_o d_{2o}\right), \end{cases} \tag{A.2}$$

and for immune persons

$$\begin{aligned} \frac{d}{dt}i &= \left(\chi_y\gamma_y + \eta_y\right)a_y + \left(\gamma_{2y} + m_y\gamma_{1y}\right)q_{1y} + \left(\gamma_{3y} + \eta_{2y}\right)q_{2y} + \gamma_{3y}q_{3y} + \left(\gamma_{2y} + \theta_y\right)d_{2y} + \\ &\quad \left(\chi_o\gamma_o + \eta_o\right)a_o + \left(\gamma_{2o} + m_o\gamma_{1o}\right)q_{1o} + \left(\gamma_{3o} + \eta_{2o}\right)q_{2o} + \gamma_{3o}q_{3o} + \left(\gamma_{2o} + \theta_o\right)d_{2o} - \\ &\quad \phi i + i\left(\alpha_y d_{2y} + \alpha_o d_{2o}\right), \end{aligned} \tag{A.3}$$

where λ is the force of infection given by equation (1) re-written as

$$\lambda = \varepsilon_{1y}\beta_{1y}a_y + \varepsilon_{2y}\beta_{2y}d_{1y} + \varepsilon_{3y}\beta_{3y}z_y q_{2y} + \varepsilon_{1o}\beta_{1o}a_o + \varepsilon_{2o}\beta_{2o}d_{1o} + \varepsilon_{3o}\beta_{3o}z_o q_{2o},$$

and

$$\sum_{j=y,o} (s_j + q_j + e_j + a_j + q_{1j} + d_{1j} + q_{2j} + d_{2j}) + i = 1,$$

which is autonomous system of equations. We remember that all classes vary with time, however their fractions attain steady state (the sum of derivatives of all classes is zero). This system of equations is not easy to determine the non-trivial (endemic) equilibrium point P^*. Hence, we restrict our analysis with respect to the trivial (disease free) equilibrium point.

The trivial or disease free equilibrium P^0 is given by

$$P^0 = \left(s_j^0, q_j^0 = 0, e_j^0 = 0, a_j^0 = 0, q_{1j}^0 = 0, d_{1j}^0 = 0, q_{2j}^0 = 0, d_{2j}^0 = 0, i^0 = 0\right),$$

for $j = y$ and o, where

$$\begin{cases} s_y^0 = \dfrac{\phi}{\phi + \varphi} \\ s_o^0 = \dfrac{\varphi}{\phi + \varphi}, \end{cases} \tag{A.4}$$

with $s_y^0 + s_o^0 = 1$.

Due to 17 equations, we do not deal with characteristic equation corresponding to Jacobian matrix evaluated at P^0, but we apply the next generation matrix theory [7].

The next generation matrix, evaluated at the trivial equilibrium P^0, is obtained considering the vector of variables $x = (e_y, a_y, d_{1y}, e_o, a_o, d_{1o})$. We apply method proposed in [24] and proved in [25]. There are control mechanisms (isolation), hence we obtain the reduced reproduction number R_r by isolation.

In order to obtain the reduced reproduction number, diagonal matrix V is considered. Hence, the vectors f and v are

$$f^T = \begin{pmatrix} \lambda s_y + e_y\left(\alpha_y d_{2y} + \alpha_o d_{2o}\right) \\ p_y \sigma_y e_y + a_y\left(\alpha_y d_{2y} + \alpha_o d_{2o}\right) \\ \left(1 - p_y\right)\sigma_y e_y + d_{1y}\left(\alpha_y d_{2y} + \alpha_o d_{2o}\right) \\ \left(1 - \chi_y\right)\gamma_y a_y + m_y \gamma_{1y} d_{1y} + \xi_y q_{3y} + q_{2y}\left(\alpha_y d_{2y} + \alpha_o d_{2o}\right) \\ \lambda \psi s_o + e_o\left(\alpha_y d_{2y} + \alpha_o d_{2o}\right) \\ p_o \sigma_o e_o + a_o\left(\alpha_y d_{2y} + \alpha_o d_{2o}\right) \\ \left(1 - p_o\right)\sigma_o e_o + d_{1o}\left(\alpha_y d_{2y} + \alpha_o d_{2o}\right) \\ \left(1 - \chi_o\right)\gamma_o a_o + m_o \gamma_{1o} d_{1o} + \xi_o q_{3o} + q_{2o}\left(\alpha_y d_{2y} + \alpha_o d_{2o}\right) \end{pmatrix} \tag{A.5}$$

and

$$v^T = \begin{pmatrix} \left(\sigma_y + \phi\right) e_y \\ \left(\gamma_y + \eta_y + \chi_y + \phi\right) a_y \\ \left(\gamma_{1y} + \eta_{1y} + \phi\right) d_{1y} \\ \left(\gamma_{3y} + \eta_{2y} + \varepsilon_{4y} + \phi\right) q_{2y} \\ \left(\sigma_o + \phi\right) e_o \\ \left(\gamma_o + \eta_o + \chi_o + \phi\right) a_o \\ \left(\gamma_{1o} + \eta_{1o} + \phi\right) d_{1o} \\ \left(\gamma_{3o} + \eta_{2o} + \varepsilon_{4o} + \phi\right) q_{2o} \end{pmatrix}, \tag{A.6}$$

where the superscript T stands for the transposition of a matrix, from which we obtain the matrices F and V (see [7]) evaluated at the trivial equilibrium P^0, which were omitted. The next generation matrix FV^{-1} is

$$FV^{-1} = \begin{bmatrix}
0 & \frac{\beta_{1y}s_y^0}{\gamma_y+\eta_y+\chi_y+\phi} & \frac{\beta_{2y}s_y^0}{\gamma_{1y}+\eta_{1y}+\phi} & \frac{\beta_{3y}z_ys_y^0}{\gamma_{3y}+\eta_{2y}+\varepsilon_{4y}+\phi} & 0 & \frac{\beta_{1o}s_y^0}{\gamma_o+\eta_o+\chi_o+\phi} & \frac{\beta_{2o}s_y^0}{\gamma_{1o}+\eta_{1o}+\phi} & \frac{\beta_{3o}z_os_y^0}{\gamma_{3o}+\eta_{2o}+\varepsilon_{4o}+\phi} \\
\frac{p_y\sigma_y}{\sigma_y+\phi} & 0 & 0 & 0 & 0 & 0 & 0 & 0 \\
\frac{(1-p_y)\sigma_y}{\sigma_y+\phi} & 0 & 0 & 0 & 0 & 0 & 0 & 0 \\
0 & \frac{(1-\chi_y)\gamma_y}{\gamma_y+\eta_y+\phi} & \frac{m_y\gamma_{1y}}{\gamma_{1y}+\eta_{1y}+\phi} & 0 & 0 & 0 & 0 & 0 \\
0 & \frac{\beta_{1y}\psi s_o^0}{\gamma_y+\eta_y+\chi_y+\phi} & \frac{\beta_{2y}\psi s_o^0}{\gamma_{1y}+\eta_{1y}+\phi} & \frac{\beta_{3y}z_y\psi s_o^0}{\gamma_{3y}+\eta_{2y}+\varepsilon_{4y}+\phi} & 0 & \frac{\beta_{1o}\psi s_o^0}{\gamma_o+\eta_o+\chi_o+\phi} & \frac{\beta_{2o}\psi s_o^0}{\gamma_{1o}+\eta_{1o}+\phi} & \frac{\beta_{3o}z_o\psi s_o^0}{\gamma_{3o}+\eta_{2o}+\varepsilon_{4o}+\phi} \\
0 & 0 & 0 & 0 & \frac{p_o\sigma_o}{\sigma_o+\phi} & 0 & 0 & 0 \\
0 & 0 & 0 & 0 & \frac{(1-p_o)\sigma_o}{\sigma_o+\phi} & 0 & 0 & 0 \\
0 & 0 & 0 & 0 & 0 & \frac{(1-\chi_o)\gamma_o}{\gamma_o+\eta_o+\phi} & \frac{m_o\gamma_{1o}}{\gamma_{1o}+\eta_{1o}+\phi} & 0
\end{bmatrix}$$

and the characteristic equation corresponding to FV^{-1} is

$$\lambda^3\left[\lambda^3 - \left(R_{1y}s_y^0 + R_{1o}s_o^0\right)\lambda - \left(R_{2y}s_y^0 + R_{2o}s_o^0\right)\right] = 0, \tag{A.7}$$

where we have

$$\begin{cases}
R_{1y} &= p_y\dfrac{\sigma_y}{\sigma_y+\phi}\dfrac{\beta_{1y}}{\gamma_y+\eta_y+\phi} + (1-p_y)\dfrac{\sigma_y}{\sigma_y+\phi}\dfrac{\beta_{2y}}{\gamma_{1y}+\eta_{1y}+\phi} \\
R_{1o} &= p_o\dfrac{\sigma_o}{\sigma_o+\phi}\dfrac{\beta_{1o}\psi}{\gamma_o+\eta_o+\phi} + (1-p_o)\dfrac{\sigma_o}{\sigma_o+\phi}\dfrac{\beta_{2o}\psi}{\gamma_{1o}+\eta_{1o}+\phi} \\
R_{2y} &= \left[p_y\dfrac{\sigma_y}{\sigma_y+\phi}(1-\chi_y)\dfrac{\gamma_y}{\gamma_y+\eta_y+\phi} + (1-p_y)\dfrac{\sigma_y}{\sigma_y+\phi}m_y\dfrac{\gamma_{1y}}{\gamma_{1y}+\eta_{1y}+\phi}\right]\dfrac{z_y\beta_{3y}}{\gamma_{3y}+\eta_{2y}+\varepsilon_{4y}+\phi} \\
R_{2o} &= \left[p_o\dfrac{\sigma_o}{\sigma_o+\phi}(1-\chi_o)\dfrac{\gamma_o}{\gamma_o+\eta_o+\phi} + (1-p_o)\dfrac{\sigma_o}{\sigma_o+\phi}m_o\dfrac{\gamma_{1o}}{\gamma_{1o}+\eta_{1o}+\phi}\right]\dfrac{z_o\beta_{3o}\psi}{\gamma_{3o}+\eta_{2o}+\varepsilon_{4o}+\phi}.
\end{cases} \tag{A.8}$$

Instead of using the spectral radius $\rho\left(FV^{-1}\right)$, which is not easy to evaluate, we apply procedure in [24] (the sum of coefficients of characteristic equation), resulting the basic reproduction number R_0 given by

$$R_0 = R_{0y} + R_{0o}, \quad \text{where} \quad \begin{cases} R_{0y} = R_y s_y^0, \\ R_{0o} = R_o s_o^0, \end{cases} \quad \text{with} \quad \begin{cases} R_y = R_{1y} + R_{2y}, \\ R_o = R_{1o} + R_{2o}, \end{cases} \tag{A.9}$$

Hence, the trivial equilibrium point P^0 is locally asymptotically stable if $R_0 < 1$.

In [22] we showed, when $z_y = z_o = 0$, that the inverse of the basic reproduction number R_0 is the fraction of susceptible persons in the steady state. But, according to [29], the inverse of the basic reproduction number R_0 given by equation (A.9) is a function of the fraction of susceptible individuals at endemic equilibrium s^* through

$$f\left(s^*, s_y^*, s_o^*\right) = \frac{1}{R_0} = \frac{1}{R_{0y}s_y^0 + R_{0o}s_o^0}, \tag{A.10}$$

where $s^* = s_y^* + s_o^*$ (see [27] [29]). For this reason, the effective reproduction number R_{ef} [26], which varies with time, can not be defined neither by $R_{ef} = R_0\left(s_y + s_o\right)$, nor $R_{ef} =$

$R_{0y}s_y + R_{0o}s_o$. The function $f(\varkappa)$ is determined by calculating the coordinates of the non-trivial equilibrium point P^*. For instance, for dengue transmission model, $f(s_1^*, s_2^*) = s_1^* \times s_2^*$, where s_1^* and s_2^* are the fractions at equilibrium of, respectively, humans and mosquitoes [27]. For tuberculosis model considering drug-sensitive and resistant strains, there is not $f(x)$, but s^* is solution of a second degree polynomial [29]. From equation (A.10), let us assume that $f\left(s^*, s_y^*, s_o^*\right) = s_y^* + s_o^*$. Then, we can define the approximated effective reproduction number R_{ef} as

$$R_{ef} = R_y s_y + R_o s_o, \tag{A.11}$$

which depends on time, and when attains steady state ($R_{ef} = 1$), we have $s^* = 1/R_0$.

The basic reproduction number R_0 is the secondary cases produced by one case of infectious person (could be anyone in one of classes harboring virus) in a completely susceptible young and elder persons without control. Let us understand R_{1j} and R_{2j}, $j = y, o$, stressing that the interpretation is the same for both subpopulations, hence we drop out subscript j. To facilitate the interpretation, we consider this infectious person in exposed class E. We assumed that hospitalized persons are not transmitting, but only asymptomatic (A), pre-diseased (D_1) and fraction of mild CoViD-19 (Q_2) persons.

1. R_1 takes into account the transmission by one person in asymptomatic A or pre-diseased D_1 class. We interpret for asymptomatic person transmitting, and between parenthesis, for pre-diseased person. One infectious person survives during the incubation period with probability $\sigma/(\sigma + \phi)$ and enters into asymptomatic class with probability p (pre-diseased, with $1 - p$) and generates, during the time $1/(\gamma + \eta + \phi)$ (pre-diseased, $1/(\gamma_1 + \eta_1 + \phi)$) staying in this class, on average $\beta_1/(\gamma + \eta + \phi)$ (pre-diseased, $\beta_2/(\gamma_1 + \eta_1 + \phi)$) secondary cases.

2. R_2 takes into account the transmission by mild CoViD-19 person. An infectious persons has two routes to reach Q_2: passing through A or D_1 (this case is given between parentheses). One infectious person survives during the incubation period with probability $\sigma/(\sigma + \phi)$ and enters into asymptomatic (pre-diseased) class with probability p (pre-diseased, with $1 - p$); survives in this class and also is not caught by test with probability $\gamma/(\gamma + \eta + \phi)$ (pre-diseased, $\gamma_1/(\gamma_1 + \eta_1 + \phi)$) and enters into mild CoViD-19 class Q_2 with probability $1 - \chi$ (pre-diseased, m); and generates, during the time $1/(\gamma_3 + \eta_2 + \varepsilon_4 + \phi)$ staying in this class, on average $z\beta_3/(\gamma_3 + \eta_2 + \varepsilon_4 + \phi)$ secondary cases.

Hence, $R_0 = R_{0y}s_y^0 + R_{0o}s_o^0$ is the overall number of secondary cases generated form one primary case introduced into a completely susceptible subpopulations of young elder persons.